Generalized Kanzaki force field of extended defects in crystals with applications to the modeling of edge dislocations

B. Gurrutxaga-Lerma*
School of Metallurgy and Materials, University of Birmingham, Elms Road, B15 2SE Birmingham, United Kingdom and Trinity College, University of Cambridge, CB2 1TQ Cambridge, United Kingdom

J. Verschueren
Department of Materials, Imperial College London, SW7 2AZ London, United Kingdom

(Received 24 February 2019; revised manuscript received 1 July 2019; published 4 November 2019)

The Kanzaki forces and their associated multipolar moments are standard ways of representing point defects in an atomistically informed way in the continuum. In this article, the Kanzaki force approach is extended to other crystalline defects. The article shows how the resulting Kanzaki force fields are to be computed for any general extended defect by first computing the relaxed defect's structure and then defining an affine mapping between the said defect structure and the original perfect lattice. This methodology can be employed to compute the Kanzaki force field of any mass-conserving defect, including dislocations, grain and twin boundaries, or cracks. Particular focus is then placed on straight edge dislocation in face-centered cubic (fcc) and body-centered cubic (bcc) pure metals, which are studied along different crystallographic directions. The particular characteristics of these force fields are discussed, drawing a distinction between the slip Kanzaki force field associated with the Volterra disregistry that characterizes the dislocation, and the core Kanzaki force field associated with the specific topology of the dislocation's core. The resulting force fields can be employed to create elastic models of the dislocation that, unlike other regularization procedures, offer a geometrically true representation of the core and the elastic fields in its environs, capturing all three-dimensional effects associated with the core.

DOI: 10.1103/PhysRevMaterials.3.113801

I. INTRODUCTION

This article concerns the representation of general crystalline defects as Kanzaki force distributions and its application to the modeling of edge dislocations. The Kanzaki forces are typically associated with point defects, where they are defined as the forces that would have to be applied on a perfect harmonic lattice to generate the point defect's displacement field [1–4]. As such, they facilitate studying the influence of the point defect in the continuum, where the Kanzaki forces, or one or more of their multipolar moment tensors [3,5,6], may be directly applied to model the point defect. In that sense, Kanzaki forces act as source terms: They are the dynamic source that generates the defect in a defect-free medium, be it a discrete harmonic lattice [3,7–9] or an elastic continuum [10,11]. Because they stem from atomistic calculations [10,12,13] but are commonly employed in the continuum and other higher level models, they can be regarded as a true multiscale modeling tool that enables transferring topological and mechanical information of the point defect from atomistic systems to higher length scales, where they have been successfully employed to study numerous phenomena involving point defects [9,10,14–20].

Recently, the authors [21] produced a formalism that extends the Kanzaki force approach to crystallographic dislocations. The use of body forces to represent dislocations has its roots in lattice dynamics studies of dislocation motion, where screw dislocations of the Volterra kind are often represented as distributed forces acting, atom by atom, across the dislocation's nominal slip plane in a perfect lattice [22–26]. Even though, in actuality, the dislocation is a topological defect characterized by a Volterra disregistry and a relaxed core [27] (and as such it can only be observed as part defective lattice [28]), in lattice dynamics models the dislocation is represented on a perfect lattice via the forces that would have to be applied on the original, defect-free lattice to generate the dislocation's topology (q.v. Refs. [7,25]).

The Kanzaki force model of screw dislocations discussed in Ref. [21] relies on characterizing the atomistic displacement map of the dislocation relative to the perfect lattice. This mapping is obtained from a structural minimization of the dislocation and its core in atomistic calculations. The Kanzaki forces are then computed in the harmonic approximation as the convolution of the force constant matrix with the atomistic displacement map. As with the Kanzaki forces of points defects, these Kanzaki forces serve as source terms: When applied on a perfect harmonic lattice, they generate the displacement field of the screw dislocation. Unlike in lattice dynamics calculations, where only Volterra screw dislocations with an infinitely thin core could be modeled [24,25], the approach discussed in Ref. [21] enabled the modeling of the dislocation core as predicted by the atomistic models, both in a harmonic lattice and in the linear elastic continuum.

*b.gurrutxagalerma.1@bham.ac.uk

This is because, as was discussed in Ref. [21], in the long wave limit the Kanzaki forces of the screw dislocation can be shown to converge to the linear elastic Burridge-Knopoff force representation [29–31] of a dislocation. This means that the Kanzaki forces can be used as source terms in the atomistic lattice or in the linear elastic continuum, thereby facilitating a linear elastic model of the core.

This article generalizes these ideas further, expanding the concept of the Kanzaki force field to any extended defect. The generalized Kanzaki force field of a defect, defined in Sec. II, is computed in a perfect crystalline lattice under the harmonic approximation and can be employed as a source term of the said defect in any lattice dynamics or lattice statics calculations, or as a source term to model the defect in the elastic continuum. As is discussed in Sec. II, the latter is true because the elastic continuum is a specific limit of the harmonic lattice approximation. In using the Kanzaki force field to model the defect in the continuum, the resulting elastic field is atomistically motivated, true to the actual topology of the defect (i.e., the geometry of the defect is directly captured by the Kanzaki force field, without recourse to approximations or simplifications) and energetically accurate within the harmonic approximation. Thus, the Kanzaki force field of a defect emerges as an attractive, simple, and very accurate way of studying crystalline defects.

As means of an example, from Sec. III onward the article focuses on studying the Kanzaki force field of edge dislocations in face-centered cubic (fcc) Cu and Al and in body-centered cubic (bcc) Ta and W. This is done because, aside from the clear interest edge dislocations have as carriers of plasticity [32], the lack of in-plane symmetries of edge dislocations means there is currently no lattice dynamics model of edge dislocations available [26]. In the past, this has meant that all lattice dynamics studies of dislocation mobility were limited to screw dislocations [22,23,25,26]. This article offers a rigorous way of extending such models to edge dislocations and, furthermore, offers a complete account of how to model the core of edge dislocations in different metals and along different crystallographic orientations in an atomistically informed way and without recourse to phenomenological regularizations such as the Peierls-Nabarro model [27]. Section V explains how to use these Kanzaki force fields to model edge dislocations in the linear elastic continuum, how to use them to obtain an unambiguous definition of the core energy that is independent of the concept of a core radius, and how to estimate core effects based on the core's multipolar moments, which are derived in the section. Section VI offers the article's closing remarks.

Albeit in the sequel the Kanzaki force field is applied to edge dislocations, the methodology described here is entirely general and can be applied to any other extended defect, as long as the harmonic lattice approximation remains acceptable. Future work will focus on studying twin and grain boundaries.

II. GENERALIZED KANZAKI FORCE FIELD

The Kanzaki force field is defined in terms of an affine mapping [33] in a crystalline lattice in the harmonic approximation. In the following, these two concepts are explained.

A. Affine mapping

Consider a perfect crystalline lattice in static equilibrium, with $\Omega_0 \subset \mathbb{R}^3$ the set of all atomic positions in the lattice. Let the equilibrium position of the kth atom in the lth unit cell of the crystal be given by $\mathbf{R}(l,k) \in \Omega_0$ relative to some reference.

Let a defect be injected in the perfect lattice Ω_0. As a result, each atom in the lattice is displaced by a certain amount off their original perfect lattice positions to their new, fully relaxed, equilibrium positions, which define $\Omega_d \subset \mathbb{R}^3$ as the set of all atomic positions in the defective lattice Ω_d. The new position of the kth atom in the lth unit cell is described with the vector $\mathbf{r}(l,k)$.

The *affine mapping* induced by the introduction of the defect on the perfect lattice is described by the displacement $\mathbf{u} : \Omega_0 \to \Omega_d$ and given by

$$\mathbf{u}(l,k) = \mathbf{r}(l,k) - \mathbf{R}(l,k). \tag{1}$$

Figure 1 shows the affine mapping associated with a dipole of straight edge dislocations.

B. Definition of the Kanzaki force field of a defect

The *Kanzaki force field* of a defect is the (fictitious) set of forces that would have to be applied on a perfect, defect-free lattice (i.e., Ω_0) to generate the same elastic field as the one attained in the defective lattice (i.e., Ω_d).

If the total potential energy of the Ω_d lattice is [34]

$$V = \sum_{l,k} \Phi[\mathbf{r}(l,k)], \tag{2}$$

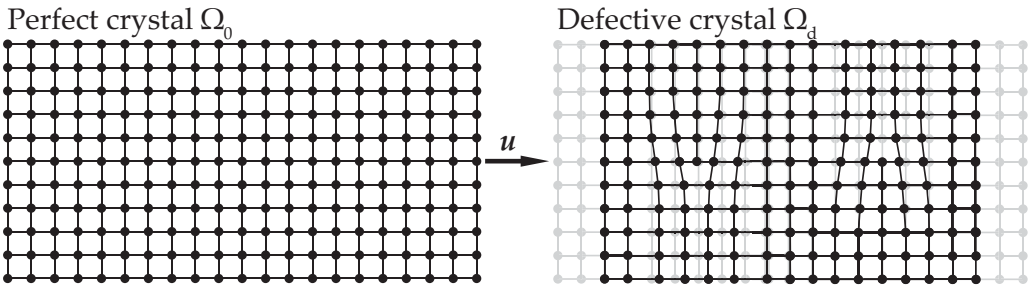

FIG. 1. Schematic of the affine mapping required to model an edge dislocation: in mapping Ω_d onto Ω_0, the number of atoms must be conserved, thereby requiring the modeling of a dipole of edge dislocations.

where $\Phi(\mathbf{x})$ is the contribution of atom (l,k) to the potential energy. The total force acting on atom (l,k) is given by

$$F_i(l,k) = -\frac{\partial V}{\partial r_i(l,k)}. \tag{3}$$

Expanding V about the defect-free Ω_0 positions leads to

$$F_i(l,k) = -\frac{1}{2}\sum_{l',k'} \left.\frac{\partial^2 \Phi}{\partial r_i(l,k)\partial r_j(l',k')}\right|_0 u_j(l',k') + \text{h.o.t.}, \tag{4}$$

where h.o.t. stands for higher order terms, the subindex 0 denotes that the derivative is evaluated at the perfect lattice positions $R(l,k)$ and $u_j(l',k') \equiv \mathbf{u}(l',k')$ is the displacement to which atom (l',k') is subjected in the affine mapping between Ω_0 and Ω_d. The need for the affine mapping is clear: Otherwise, the expansion of the defective lattice's potential energy about the perfect lattice positions is ill defined.

If the displacement of the atoms off their perfect lattice Ω_0 positions is small, one may invoke the *harmonic approximation* and neglect all higher order contributions to Eq. (4) [34,35]. In that case,

$$F_i(l,k) = -\sum_{l',k'} \Phi_{ij}(l-l',k-k')u_j(l',k'), \tag{5}$$

where

$$\Phi_{ij}(l,l';k,k') \equiv \left.\frac{1}{2}\frac{\partial^2 \Phi}{\partial r_i(l,k)\partial r_j(l',k')}\right|_0 \tag{6}$$

is the force constant matrix [34,35] of the perfect Ω_0 lattice. Since Ω_0 is a perfect lattice, it is bound by translational symmetry, $\Phi_{ij}(l,l';k,k') = \Phi_{ij}(l-l',k-k')$ [34], among some other properties (q.v. Refs. [34,35]).

The Kanzaki force field $\mathbf{f}^K$ associated with the $\mathbf{u}:\Omega_0 \to \Omega_d$ affine mapping is then defined as

$$f_i^K(l,k) = -\sum_{l',k'} \Phi_{ij}(l-l',k-k')\mathbf{u}_j(l',k'). \tag{7}$$

The Kanzaki force field given by Eq. (7) can be used as a source term on a perfect harmonic lattice, as they generate the same displacement field as that observed in Ω_d. However, the converse is not necessarily true: The Kanzaki field need not be applied with reverse sign on the atoms of the defective lattice Ω_d to restore the perfect lattice Ω_0. This is because the force constant matrix of the defective lattice is not the same as that of the perfect lattice nor has the same symmetries. Further comments on this may be found in the Supplemental Material [36], which collect a number of accessory remarks about the validity of the Kanzaki force field method. In particular, the Supplemental Material shows that the Kanzaki force field can be employed in a linear elastic continuum because in the long wave limit it converges to the Burridge-Knopoff force representation of the corresponding defect. The Supplemental Material also shows that the potential energy associated with the Kanzaki force field of a defect is the harmonic lattice's potential energy, so that the energy error associated with the Kanzaki force field is the anharmonic correction energy term (cf. Ref. [34]).

III. COMPUTATION OF THE KANZAKI FORCE FIELD

This section details how to compute the Kanzaki force field of a defect as was defined in Sec. II. Equation (7) defines the Kanzaki force field of a defect as the product of the affine mapping $\mathbf{u}(\mathbf{x}):\Omega_0 \to \Omega_d$ with the perfect lattice's force constant matrix. Thus, computing the Kanzaki force field of a defect entails two distinct steps: (1) computing the actual affine mapping and (2) performing the product defined in Eq. (7), which requires calculating the perfect lattice's force constant matrix.

In the following, focus is placed on studying edge dislocations in a number of cubic metals using phenomenological interatomic force fields. Edge dislocations are eminently useful in the description of plastic flow in metals [27,32] and enable an almost immediate comparison between the Kanzaki force field description of the defect and more traditional descriptions such as the Volterra dislocation. In fcc metals, they also offer the possibility of studying stacking faults at the same time, since the dislocation core dissociates into Shockley partials [27]. Furthermore, no clear lattice statics force model of an edge dislocation is available in the literature—this work serves to fill that gap.

Two observations must be made: First, both the affine mapping and the force constant matrix computation are achievable using a vast number of atomistic techniques, ranging from inherently quantum mechanical calculations such as density functional theory (DFT) [37] to classical calculations based on phenomenological interatomic force fields [38].

Second, the definition of the Kanzaki force field is entirely general, and may be applied to the study of any defect for which an affine mapping may be found. The main limitation of the approach lies in its reliance on the harmonic approximation. Although the defect's relaxed structure and affine mappings may be obtained by capturing higher order effects, particularly if it is computed with DFT or anharmonic interatomic potentials, the ensuing Kanzaki force field is inherently harmonic, and it will not capture third or higher anharmonicities, which would be of interest, for instance, in capturing thermal effects or phase transitions associated with the defect (see Refs. [34,39]). Still, for any defect that may be wished to be modeled using continuum elasticity, be it first or second order [40,41], local or nonlocal [42,43], the Kanzaki force field of the defect given by Eq. (7) offers an exact account of the associated elastic fields. This appears to hold true for the study of a vast number of extended defects, including crystallographic dislocations [27,44], cracks [45], stacking faults [27], or twin boundaries and low-angle grain boundaries [46], among other extended defects.

A. Computation of the affine map of a straight edge dislocation

Affine maps of dislocations are commonly computed in the context of the core structure of screw dislocations, particularly of bcc metals [47–50], where the associated concept of differential displacement map is employed in determining properties associated with dislocation motion and plastic slip, such as the Peierls barrier [27,47]. The computation of the affine map induced by an edge dislocation is less common and here arises as the first step towards computing the full Kanzaki force field of an edge dislocation.

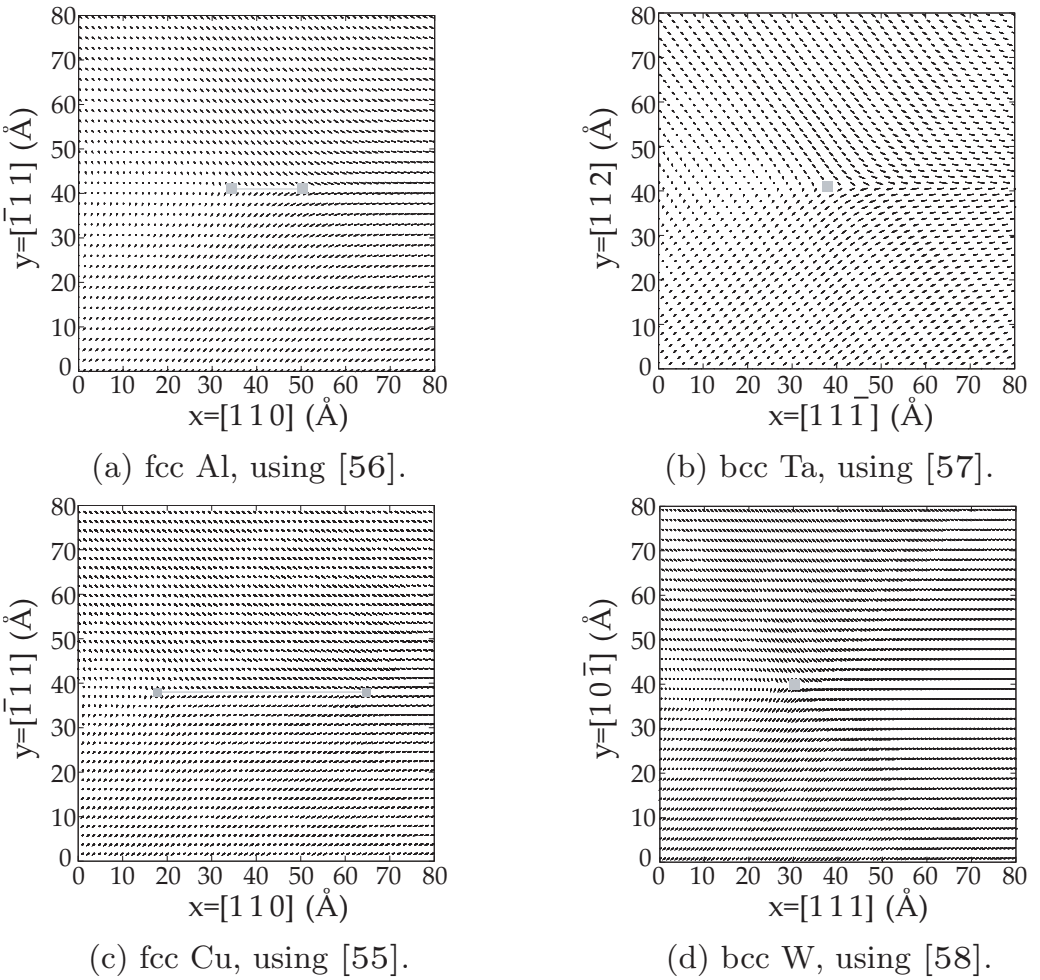

FIG. 2. Affine maps of different edge dislocations, centered about the dislocation core. The topological location of the dislocation line (or of the dislocation partials) was determined using the DXA algorithm [59] as implemented in Ovito [60] and is indicated here with a gray square. The displacement vectors are applied on the perfect lattice position and indicate the final location of the corresponding atom. The original box size was 200 × 100 × 10 unit cells for both Al and Cu and 160 × 100 × 12 unit cells for Ta and W.

All calculations reported here begin with a perfect lattice, which is minimized in LAMMPS [51] under an appropriate interatomic force field to obtain Ω_0. The system consists of a sufficiently large simulation box subjected to periodic boundary conditions in all three directions. Once the perfect lattice is minimized, a dipole of edge dislocations is injected into the systems, centered about the middle of the simulation box. The dipole is necessary to ensure that mass is conserved upon injecting the edge dislocation and that therefore the affine map on the lattice can be defined. The dipole is injected by slipping a $\pm\mathbf{B}/2$ all atoms above (below) the nominal slip surface in the appropriate direction of slip; the slipped surface occupies half the nominal x distance of the simulation box, which is therefore made to be sufficiently large to ensure that the two dislocations in the dipole do not mutually annihilate. Then the system is minimized in LAMMPS, resulting in a minimized dipole of edge dislocations that defines the Ω_d defective lattice. The affine mapping is then computed performing a nearest neighbor search atom by atom between the original Ω_0 and defective Ω_d lattices. In this work, this was achieved by constructing a well-balanced k-d tree [52] containing Ω_0 and Ω_d, which was implemented using the nanoflann library [53].

In the following, the Kanzaki force fields of four cubic metals will be computed: fcc Cu and fcc Al, as exponents of two fcc metals of very dissimilar stacking fault energies, and bcc W and bcc Ta, with different crystallographic directions for the slip surface. Four well-known embedded atom potentials [54] were used: for Cu, Ref. [55]; for fcc Al, Ref. [56]; for bcc Ta, Ref. [57]; and for bcc W, Ref. [58]. The box sizes were 200 × 100 × 10 unit cells with crystallography $[1\,1\,0] \times [\bar{1}\,1\,1] \times [1\,\bar{1}\,2]$ for both fcc metals, and 160 × 100 × 12 for both bcc metals, with crystallography $[1\,1\,\bar{1}] \times [\bar{1}\,1\,2] \times [\bar{1}\,1\,0]$ for Ta and $[1\,1\,1] \times [1\,0\,\bar{1}] \times [1\,\bar{2}\,1]$ for W.

Figure 2 collects the affine maps resulting from the different lattice minimisations we report in this article, centered about the core of the leftmost of the two dislocations, the geometric center of which is indicated in the figure. It depicts the true magnitude $\mathbf{u}(l, k)$ displacement applied on the Ω_0 perfect lattice atomic positions. As may be seen, the magnitude of the affine mapping is not quantized about the dislocation core, but away from it, it quickly approaches the crystallographic magnitudes of either 0 (to the left of the core) or $\pm B$ (to the right of the core, where the slip plane lies).

B. Computation of the Kanzaki force field

Once the affine mapping has been obtained, the Kanzaki force field may be computed using Eq. (7). This requires computing the force constant matrix. In the computations reported here, this is done from an embedded atom interatomic force field.

For the embedded atom potentials, the force constant matrix has a well-known form (see Ref. [61]), so its computation will not be reproduced here. The product between the force constant matrix and the affine mapping was performed using an in-house code that relies on the Eigen linear algebra library [62].

IV. SLIP AND CORE KANZAKI FIELDS OF AN EDGE DISLOCATION

The result of applying Eq. (7) to the affine mapping $\mathbf{u}(l,k)$ of an energy minimized structure such as the ones shown in Fig. 2 will hereafter be called the *full Kanzaki force field*, to emphasize the fact that it captures both the relaxed topology of the core and the crystallographical disregistry that characterizes the dislocation away from the core.

The full Kanzaki force field can be divided by linear superposition into the *slip* and *core* Kanzaki force fields [21]. The *slip Kanzaki force field* is the field necessary to produce the topology of a Volterra dislocation in the dislocated lattice, without further provisions for the relaxation of the lattice about the dislocation core. The affine mapping in that case can be directly given mathematically as [21]

$$u_i^{\text{slip}}(l,k) = \chi_s(l-l',k'k')B_i, \tag{8}$$

where $B_i \equiv \mathbf{B}$ is the dislocation's Burgers vector and χ_s is a choice function of the form [21,26]

$$\chi_S(l-l',k-k') = \begin{cases} +1 & \text{if } (l,k) \text{ is above the slip surface and } (l',k') \text{ below} \\ -1 & \text{if } (l,k) \text{ is below the slip surface and } (l',k') \text{ above} \\ 0 & \text{otherwise} \end{cases}. \tag{9}$$

The corresponding *slip Kanzaki forces* are therefore

$$f_i^{\text{slip}}(l,k) = -\sum_{l',k'} \Phi_{ij}(l-l',k-k')B_j\chi_s(l-l',k'k') \tag{10}$$

and can be computed analytically, without recourse to an energy minimization of the sort described in Sec. III A.

Given that the Kanzaki force field is defined in a harmonic lattice, the slip Kanzaki force field can always be regarded as a constituent part of the full Kanzaki force field. The difference between the full Kanzaki force field and the slip Kanzaki force field is the *core Kanzaki force field*, which accounts for core effects missed in the definition of the Volterra dislocation.

Core effects encompass all those effects missed in the Volterra model of a dislocation, but that can be modeled in the atomistic system. In particular, the topology of the core will deviate from the infinitely thin core of a Volterra dislocation; the actual core will have a finite width and the atomic arrangement about it will be distorted relative to the perfect lattice position [27]. The core Kanzaki force field is hereafter defined as

$$f_i^{\text{core}}(l,k) = f_i^K(l,k) - f_i^{\text{slip}}(l,k), \tag{11}$$

that is, the difference between the actual relaxed affine mapping and the displacement field necessary to inject a Volterra dislocation in the lattice instead. As said, because in the far field the relaxed lattice Ω_d is defined by a Volterra displacement field [so that away from the core $\mathbf{u}(l,k) \approx \mathbf{u}^{\text{slip}}(l,k)$], here $\mathbf{u}^{\text{core}}$ acts as a measure of the relative displacement of the atoms at the dislocation core.

We adopt the following convention: The Volterra displacement (and the slip Kanzaki forces) is applied on the geometrical center of the corresponding stacking fault. In all other cases, the Volterra displacement field is applied on the atoms placed immediately above and below the geometrical location of the dislocation line.

A. Computational results for the Kanzaki force field of edge dislocations in Al, Cu, Ta, and W

Using the procedure outlined in Sec. III B, the Kanzaki force fields for an edge dislocation in fcc Al and Cu, and in bcc Ta and W, were computed and collected in Fig. 3, which depicts the total Kanzaki force (i.e., including both slip and core components), along the crystallographic directions defined in Fig. 2 for the corresponding affine maps of the same materials. Two effects are observed, which merit separate treatment in the following.

1. Slip force field

Away from the core, the Kanzaki force field is composed of force doublets acting across the slip plane in the atomic planes immediately above and below it. These forces appear in all four materials (with a particular proviso for $1/2\{1\,1\,2\}\langle 1\,1\,1\rangle$ edge dislocations in bcc metals, which is discussed in more detail below) and arise because of the relative $\pm B$ slip displacement that, away from the core, characterizes the dislocation as a Volterra disregistry.

This is confirmed in Fig. 4, which shows the Volterra contribution to the Kanzaki force field for each of the metals considered. The Volterra contribution is computed using Eq. (10) (i.e., by injecting a pure Volterra dislocation into the lattice); this entails imposing a relative displacement $u_x = \pm B/2$ for all the atoms immediately above and below the nominal slip surface. No provision is made for the core, which as in the Volterra dislocation is assumed to be infinitely thin. The resulting slip Kanzaki force field consists largely of two components: a set of force doublets acting across the slip plane and a net resultant vertical force acting at the nominal core. As is discussed in Sec. V A, these two sets of forces have well-defined magnitudes.

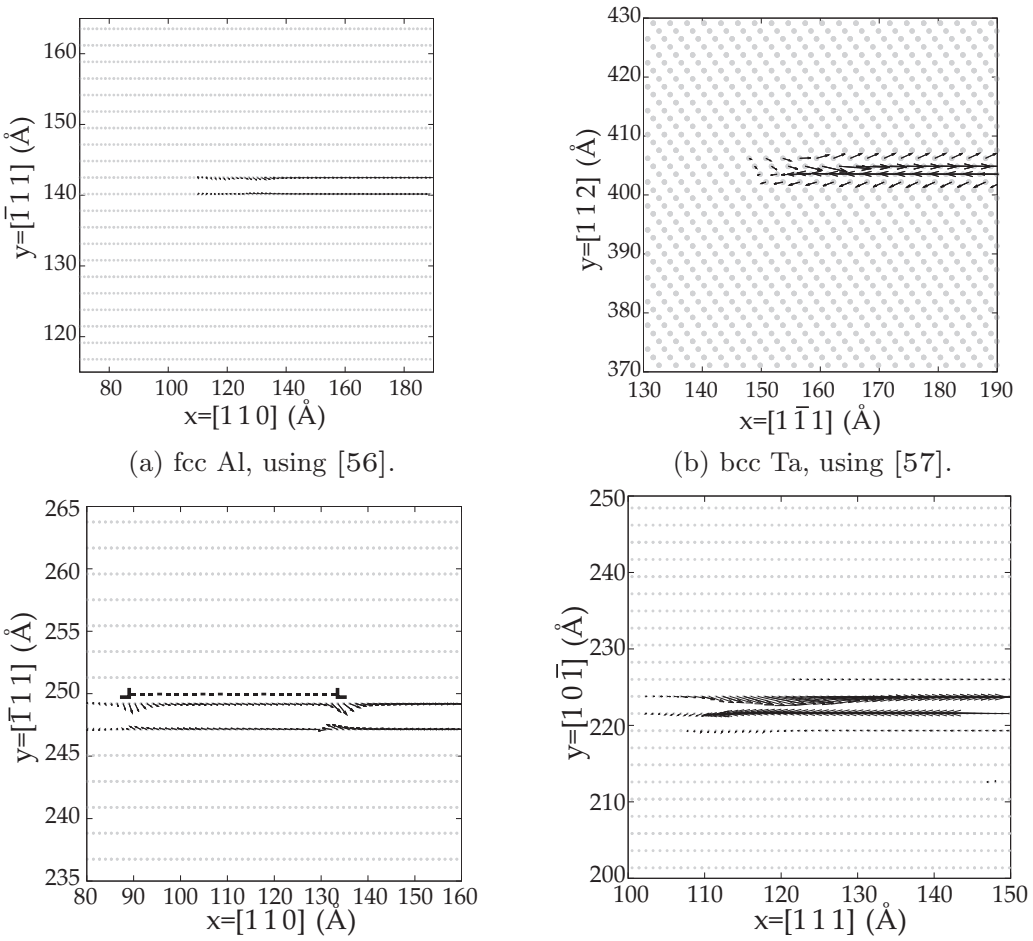

(a) fcc Al, using [56]. (b) bcc Ta, using [57].

(c) fcc Cu, using [55]. (d) bcc W, using [58].

FIG. 3. Kanzaki core fields corresponding to the affine maps in Fig. 2. The scale for the forces is 1 Å ≡ 1eV/Å.

2. *Core Kanzaki force field*

The core Kanzaki fields of these systems are reproduced in Fig. 5. As may be seen, they are generally localized about the topological position of the dislocation line.

In particular, for the fcc metals, the core field is distributed along the stacking fault lying at the dislocation core. This means that the core field is highly localized for high stacking fault energy metals, as is the case of fcc Al [Fig. 5(a)], but widely extended for low stacking fault energy metals such as fcc Cu, where it is extended over ≈50 Å. The magnitude of the core forces is also weaker than the slip forces: Excluding the f_y central force component, which is due to the slip field, they are about one order of magnitude weaker (i.e., ≈0.1eV/Å).

For bcc metals, the core is generally more localized than for fcc metals. This is readily observable in the case of Ta [Fig. 5(b)]. For bcc W in Fig. 5(d), the core appears more extended; however, considering the large magnitude of the slip Kanzaki forces in W (in excess of 7.5eV/Å), the W core forces shown in Fig. 5(d) are about two orders of magnitude smaller (≈0.1eV/Å).

Except for bcc Ta, the slip Kanzaki forces away from the core act only in the x direction. Tantalum, however, shows the presence of an additional set of f_y doublets acting across the $\langle 1\,1\,2\rangle$ slip surface. This is an unexpected feature of edge dislocations in some specific crystallographic alignments of bcc lattices. As is discussed in Sec. V, the continuum level expectation for the slip forces is that they be formed by force doublets acting across the slip plane in the x direction. In the case of bcc Ta, however, an additional set of f_y doublets in the y direction appears.

These f_y doublets originate due to the nondiagonal terms of the force constant matrix for the $\langle 1\,1\,2\rangle$ crystallographic orientation [63] in bcc metals and are, therefore, heavily dependent on the exact nature of the interatomic force field (see Ref. [64]). Similar behavior (not presented here) was also observed in bcc Fe or bcc W for the same $1/2\langle 1\,1\,1\rangle\{1\,1\,2\}$ edge dislocations. Notice, however, that the $1/2\{1\,1\,1\}\langle 1\,1\,0\rangle$ edge dislocation in bcc W does not display these f_y doublets—this is also the case for bcc Ta or bcc Fe in the same orientations.

The effect of the f_y doublets is to promote the curvature of the slip plane, previously reported for bcc metals [65].

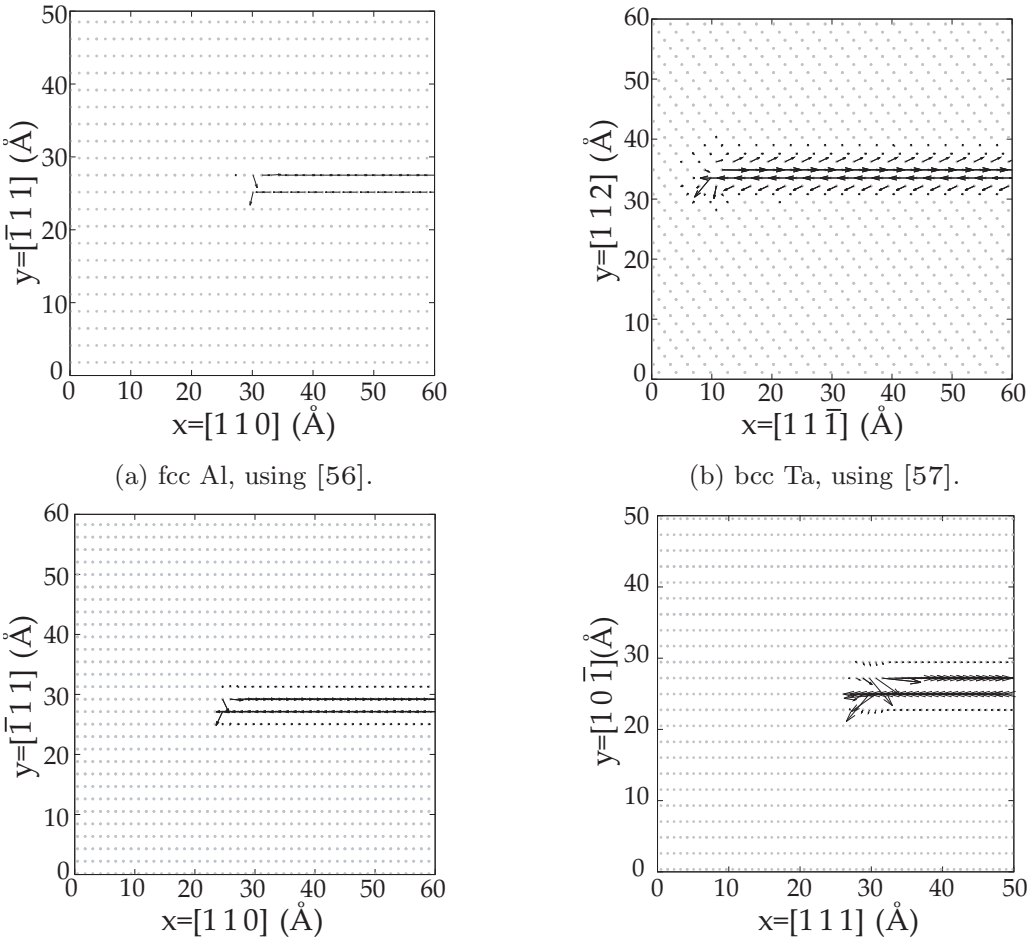

(a) fcc Al, using [56].

(b) bcc Ta, using [57].

(c) fcc Cu, using [55].

(d) bcc W, using [58].

FIG. 4. Volterra Kanzaki forces for the reference materials. Scale 1 Å ≡ 1eV/Å.

The curvature can be observed in Fig. 6, which shows the $u_y(l,k)$ displacement field component experienced by the atoms immediately above the slip surface about the nominal position of the core. As can be seen, the atoms experience a logarithmic decay away from the core, which is characteristic of the Volterra dislocation [27]. However, unlike in the classical Volterra solution, the decay at either side of the core is asymmetric. This is related to the curvature on the {112} plane and can be understood in terms of the f_y doublets in the linear elastic continuum. The curvature does not translate in a change in the Peach-Koehler force, so it is not expected to affect the dislocation motion.

Thus, consider a dipole of edge dislocations separated a distance L similar to the one that has been simulated here. In the linear elastic continuum, the dipoles may be subsumed to a distribution of force doublets of the form

$$f_y(x,y) = f_0\delta'(y)[H(x) - H(x-L)], \tag{12}$$

where x is the slip direction and y the slip plane normal, and where f_0 is the doublet's magnitude, which in the case of Ta we report here is about $0.1457\mu B$. The elastic field associated with these doublets can be found via the representation theorem [66]

$$\begin{aligned} u_x^{f_y}(x,y) &= \int_{\mathbb{R}\times\mathbb{R}} f_0 G_{xy}(x-x',y-y')f_y(x',y')dx'dy' \\ &= -\int_0^L f_0 G_{xy,y}(x-x',y)dx', \\ u_y^{f_y}(x,y) &= \int_{\mathbb{R}\times\mathbb{R}} f_0 G_{yy}(x-x',y-y')f_y(x',y')dx'dy' \\ &= -\int_0^L f_0 G_{yy,y}(x-x',y)dx', \end{aligned} \tag{13}$$

where $G_{ij}(x,y)$ is the planar elastic Green's function [67]

$$\begin{aligned} G_{xy}(x,y) &= \frac{xy}{8\pi\mu(1-\nu)r^2}, \\ G_{yy}(x,y) &= \frac{1}{8\pi\mu(1-\nu)}\left[\frac{y^2}{x^2+y^2} - (3-4\nu)\log(r^2)\right], \\ r &= \sqrt{x^2+y^2}. \end{aligned} \tag{14}$$

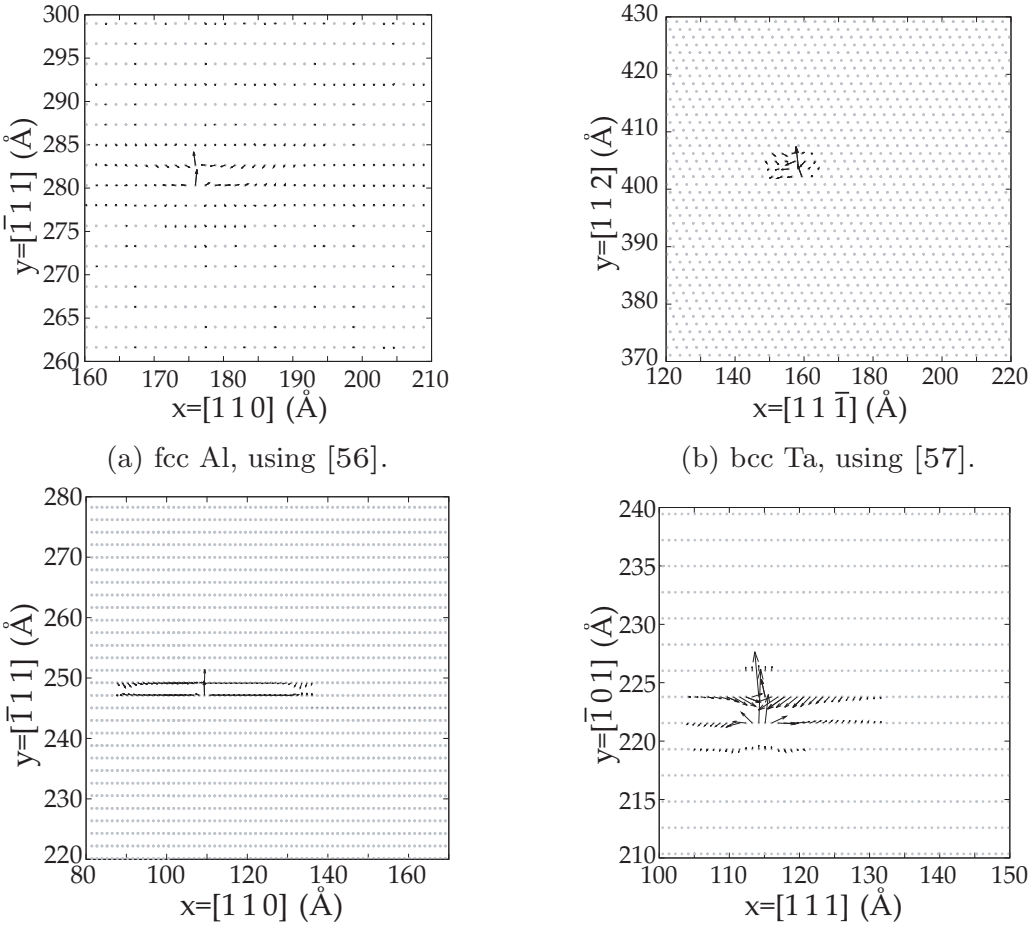

(a) fcc Al, using [56]. (b) bcc Ta, using [57].

(c) fcc Cu, using [55]. (d) bcc W, using [58].

FIG. 5. Core Kanzaki forces for the reference materials. Scale of 1 Å ≡ 1eV/Å.

The convolution results in

$$u_x^{f_y}(x,y) = \frac{f_0}{8\pi\mu(\nu-1)}\left[y^2\left(\frac{1}{(L-x)^2+y^2}-\frac{1}{x^2+y^2}\right) + \log\left(\frac{(L-x)^2+y^2}{x^2+y^2}\right)\right], \tag{15}$$

$$u_y^{f_y}(x,y) = \frac{f_0}{8\pi\mu(\nu-1)}\left\{y\left(\frac{L-x}{(L-x)^2+y^2}+\frac{x}{x^2+y^2}\right) -2(2\nu-1)\left[\tan^{-1}\left(\frac{L-x}{y}\right)+\tan^{-1}\left(\frac{x}{y}\right)\right]\right\}. \tag{16}$$

These two displacement field components are superposed to the Volterra dislocation's, which as discussed in Ref. [21] are generated by the f_x force doublets and a net resultant f_y acting at the core. Their effect is one of curving the slip plane and the dislocation.

Figure 6 shows the u_y displacement field component for the atoms immediately above the slip plane, at either side of the core, the position of which is marked with a vertical line. The figure displays the displacement field predicted by the Volterra dislocation and that predicted by the model corrected with Eq. (16) to include the f_y doublets' contribution. As can be seen, the Volterra field is symmetric about

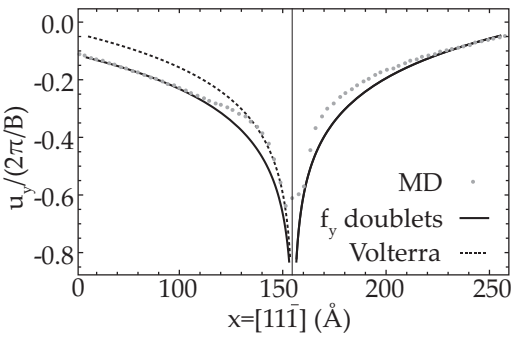

FIG. 6. u_y displacement field component in the atomic row immediately above the slip plane in bcc Ta. The figure compares the atomistic displacement field ('MD') with the displacement field accounting for the f_y doublets acting across the slip plane, and the classical Volterra solution, which is symmetric about the core, here marked with a vertical line.

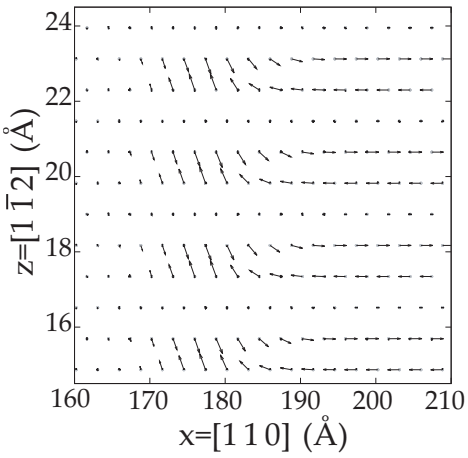

(a) (f_x, f_z) Kanzaki force field distribution in the slip plane for fcc Al.

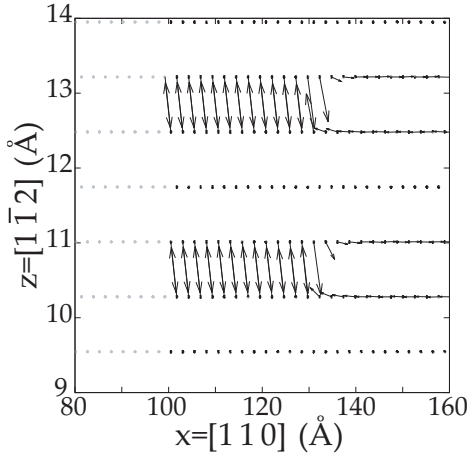

(b) (f_x, f_z) Kanzaki force field distribution in the slip plane for fcc Cu.

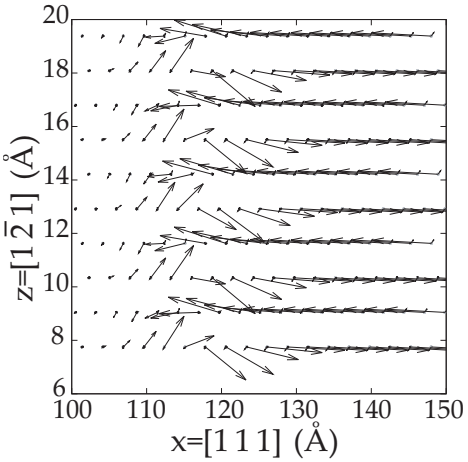

(c) (f_x, f_z) Kanzaki force field distribution in the slip plane for bcc W.

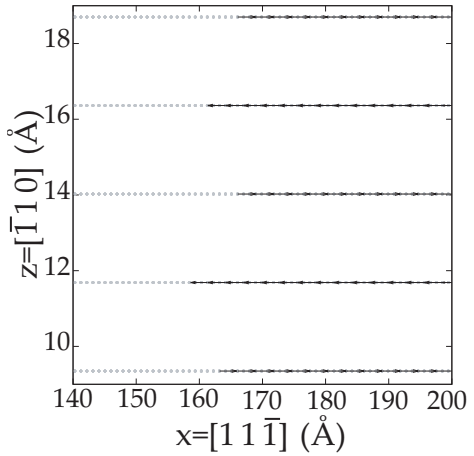

(d) (f_x, f_z) Kanzaki force field distribution in the slip plane for bcc Ta.

FIG. 7. Antiplanar Kanzaki field components. The scale is 1 Å ≡ 1 eV/Å, except for Fig. 7(d), where the scale is 1 Å ≡ 2 eV/Å.

the core, whereas the atomistic calculation's is not; upon adding the correction due to the f_y doublets, the asymmetry is obtained. This asymmetry and the ensuing curvature can also be appreciated in Fig. 4 in the Supplemental Material, which compares the atomistic and linear elastic planar stress field components for this very same dislocation.

The presence of the force doublets suggests that, unlike in the pure Volterra description, the orientation of the slip plane can affect the elastic fields of the dislocation, and that there are specific crystallographic orientations where the dislocation is considerably non-Volterra even away from the core. For instance, here we have seen that an edge dislocation slipping on the {1 1 2} planes in a bcc metal has an additional extended f_y component that is not present if the dislocation is slips on {1 1 0} planes (as is shown here for bcc W). This effect is relatively small because the f_y doublet magnitudes are about one order of magnitude smaller than the f_x doublets that generate the Volterra dislocation; however, unlike other *core effects*, it is not localized about the core, so the long-range effects will be larger than any deviation of the stress fields due to the core structure.

3. Antiplanar Kanzaki force components

The core Kanzaki force field of edge dislocations may also contains antiplanar force components acting on the z direction. By antiplanar, we mean that the core forces act in the antiplanar (z) direction, meaning that the core itself needs to be represented in three dimensions. These f_z components are entirely missed in the Volterra dislocation and other descriptions of the dislocation core such as the Peierls-Nabarro model (see Ref. [27]). In the Kanzaki force field, such three-dimensional effects are captured by default.

For fcc metals, the antiplanar forces are associated with the intrinsic stacking fault that conforms the dissociated core. For bcc metals where there is no stacking, they may or may not be present, depending on the crystallographic orientation of the third dimension.

Figure 7 collects the antiplanar force components as part of the full Kanzaki force field. This is done so as to illustrate a number of three-dimensional effects arising due to the complex nature of the dislocation. First, as may be seen in Figs. 7(a) and 7(b), in fcc metals the slip Kanzaki forces (i.e., the force components acting in the x direction)

act only on four of the six planes that conform to the *ABCDEFABCDEF* ... stacking sequence (cf. Ref. [27]). Two of the said six planes lack Kanzaki forces, in spite of the fact that the atoms on the plane do experience a relative displacement. This is due to the predicted interactions between atoms belonging to different planes in the stacking sequence: The Kanzaki force field in Eq. (7) is not the result of a simple matrix product, but relies on the long-range interactions of each atom with the rest. This does not arise in the bcc metals, where no stacking exists, and as a result slip forces act with alternating sign on each atomic plane [see Figs. 7(c) and 7(d)].

The antiplanar force component itself acts due to the presence of the intrinsic stacking fault acting at the core, which alters the stacking sequence there. Indeed, the f_z forces act periodically in alternating rows that match the stacking fault proper and point in the direction of the next atomic plane in the stacking sequence. In both the Cu and Al cases, they have a very similar form of equal and opposite forces acting along the line that joins the atoms in the (intrinsic) stacking fault; due to the sequence in the stacking of the three distinct atomic planes, one in each third atomic plane experiences no antiplanar Kanzaki force [see Figs. 7(a) and 7(b)].

For bcc metals, the antiplanar forces do not exist for the case of the $\langle 1\,1\,1\rangle\{1\,1\,2\}$ edge dislocation in Ta. However, for the $\langle 1\,1\,1\rangle\{1\,1\,0\}$ edge dislocation in W, the antiplanar forces are not negligible. In this case, the antiplanar force components arise due to the nondiagonal nature of the force constant matrix along the $\langle 1\,1\,2\rangle$ directions, which was responsible for the f_y force doublets in the case of the $\langle 1\,1\,1\rangle\{1\,1\,2\}$ edge dislocation in Ta. Again, the presence of antiplanar forces in bcc metals suggests that there exists a long-range deviation between the Volterra dislocation's fields and the actual fields of dislocations in bcc metals, brought about by the slip plane under consideration: Edge dislocations with slip on $\{1\,1\,2\}$ planes will not have antiplanar core components; edge dislocations with slip on $\{1\,1\,0\}$ planes will.

Nevertheless, the antiplanar core components highlight that despite being a relatively common assumption [27,61], the core of edge dislocations is inherently nonplanar for a wide range of metals and orientations. Our current calculations show that the core of all edge dislocations in fcc metals is bound to be nonplanar due to the presence of the intrinsic stacking fault, which carries additional antiplanar force components. In bcc metals, the nonplanarity is dependent on the specific crystallographic orientation of the slip surface and the Burgers vector: Here we have found that $\langle 1\,1\,1\rangle\{1\,1\,0\}$ edge dislocations in bcc metals will have a nonplanar core, whereas the core of $\langle 1\,1\,1\rangle\{1\,1\,2\}$ edge dislocations in bcc metals will likely be strictly planar. It is worth, however, pointing out that nonplanar effects will be relevant in short-range interactions. Indeed, the magnitude of the antiplanar Kanzaki force components is, for all metals considered here, of the order of $0.1\mathrm{eV/\AA}$, i.e., about an order of magnitude weaker than the Volterra slip forces—even for bcc W, the largest f_z component is $\approx 0.5\mathrm{eV/\AA}$. Thus, although the antiplanar forces add an additional set of localized and relatively weak antiplanar elastic field components to the dislocation which are not available in the Volterra or Peierls-Nabarro descriptions of edge dislocations, their effect will be extremely localized, and relatively weak compared to the in-plane stress field components.

V. ELASTIC MODELS OF THE EDGE DISLOCATION BASED ON THE KANZAKI FORCE FIELD

As with point defects [11] and screw dislocations [21], the Kanzaki force field of edge dislocations can be employed as a source term in the linear elastic continuum. This allows the direct translation of the detailed topology of the defect to the linear elastic continuum, and a better modeling of its long- and short-range effects. This invariably results in models of the dislocation where the core's width and general topology (and energy) in the continuum match the atomistic prediction.

A. Volterra edge dislocation and the slip Kanzaki force field

As has been noted in Sec. III B, all the Kanzaki force fields can be divided into core and slip force components. The slip force field is characterized by a set of force doublets acting across the slop surface, and a net resultant force acting at the dislocation core in the normal direction to the slip plane. These two forces correspond with the Burridge-Knopoff force representation of an edge dislocation in the linear elastic continuum.

According to the Burridge-Knopoff theorem, any displacement discontinuity $[u_i](\mathbf{x})$ compactly supported over some surface D might be represented as a set of equivalent body forces, given by

$$f_p(\mathbf{x}) = -\int_{D'} C_{ijpq}\nu_j[u_i](\mathbf{x}-\mathbf{x}')\partial_q\delta(\mathbf{x}-\mathbf{x}')dD', \qquad (17)$$

where C_{ijpq} is the elastic constants tensor and D is the slip surface, the normal vector of which is ν_j. For a straight edge dislocation, $u_1(\mathbf{x}) = BH(x_1)\delta(x_2)$, for B the Burgers vector, whereupon for a linear isotropic material

$$f_1(x,y) = -B\mu\mathrm{H}(x_1)\delta'(x_2),\ f_2(x,y) = -B\mu\delta(x_1)\delta(x_2). \qquad (18)$$

This represents a distribution of force doublets in the $x_1 \equiv x$ direction, and a force singleton acting at the position of the dislocation line. As may be seen in Fig. 4, the slip Kanzaki force field clearly displays these two components: a vertical force acting at the core, and a distribution of force doublets acting across the slip surface.

The force doublets acting across the slip plane in the crystalline lattice may be directly assimilated to the Burridge-Knopoff force doublets, since in the linear elastic limit of the harmonic lattice the planes immediately above and below the nominal slip surface are subsumed into the notional continuum slip surface [21]. The magnitude of the computed slip Kanzaki force doublets are also in good agreement with the Burridge-Knopoff magnitude of BC_{12} (or $B\mu$) for each material. The Supplemental Material collects the numerical verification of this.

B. Elastic model of the dislocation: The core Kanzaki field

In addition to the slip forces that on their own generate the Volterra dislocation, the dislocation core may also be

modeled in the continuum using the core Kanzaki force field as source terms. Thus, let f_i^{core} be the set of Kanzaki core forces, represented in Fig. 5 and defined as the difference between the full Kanzaki field of the relaxed dislocation and the Kanzaki field of the Volterra dislocation. They may be expressed as a distribution of point forces,

$$f_i^{\text{core}}(\mathbf{x}) = \sum_n f_i^n \delta(\mathbf{x} - \mathbf{x}_n), \tag{19}$$

where f_i^n is the magnitude of each individual core force component, applied on point $\mathbf{x}_n$.

As has been established above, the slip forces can be described using the Burridge-Knopoff force representation in the continuum, i.e., as a continuous distribution of slip,

$$f_i^{\text{slip}}(\mathbf{x}) = -B_j \nu_l C_{ikjl} \partial_k H(x_1)\delta(x_2). \tag{20}$$

Given that the core field is defined as the difference between the global Kanzaki force field and the slip Kanzaki force field, the sum $f_i^{\text{core}} + f_i^{\text{slip}}$ may be employed as a source term in the elastic continuum to represent the whole dislocation.

The source representation theorem states that the elastic field associated with $f_i^{\text{core}} + f_i^{\text{slip}}$ will be [11]

$$u_i(\mathbf{x}) = \int_{\mathbb{R}^3} G_{ij}(\mathbf{x} - \mathbf{x}')\left[f_i^{\text{core}} + f_j^{\text{slip}}\right] d\mathbf{x}' \tag{21}$$

for $G_{ij}(\mathbf{x})$ the linear elastic Green's function (cf. Ref. [67]). In this case, f_i^{slip} generates the linear elastic field of a Volterra dislocation, $u_i(\mathbf{x})^{\text{slip}}$. It takes the familiar analytic form of the elastic fields of an edge dislocation (see Refs. [11,67]).

The core elastic field is then given by

$$u_i^{\text{core}}(\mathbf{x}) = \sum_n f_j^n G_{ij}(\mathbf{x} - \mathbf{x}_n). \tag{22}$$

Thus, using the core Kanzaki field in combination, an elastic model of the dislocation may be produced, one where the relaxed core's geometry is properly captured via the core Kanzaki field. The displacement field of this *corrected* model is

$$u_i^{\text{corr}}(\mathbf{x}) = u_i^{\text{Volt}}(\mathbf{x}) + u_i^{\text{core}}(\mathbf{x}), \tag{23}$$

where $u_i^{\text{Volt}}(\mathbf{x})$ is the displacement field of a Volterra dislocation (q.v. Ref. [27]), and the corrected stress fields may then be obtained from Hooke's law, as

$$\begin{aligned}\sigma_{ij}^{\text{corr}}(\mathbf{x}) &= C_{ijpq}\tfrac{1}{2}\left(u_{p,q}^{\text{corr}} + u_{q,p}^{\text{corr}}\right) \\ &= \sigma_{ij}^{\text{slip}} + \sigma_{ij}^{\text{core}},\end{aligned} \tag{24}$$

where

$$\sigma_{ij}^{\text{core}} = C_{ijpq} \sum_n f_k^n G_{pk,q}(\mathbf{x} - \mathbf{x}_n) \tag{25}$$

and where $G_{pk,q}(\mathbf{x})$ has a well-known explicit form (see Ref. [67]).

C. Multipolar expansions of the dislocation core

The length scales over which core effects are relevant can be estimated by computing the core's multipolar moments. The multipolar moments would seek to substitute the extended core's force field by a set of force dipoles, quadrupoles, octopoles, etc., that accurately approximate the long-range effects of the core's Kanzaki force field. Thus, the multipolar moments could be envisioned to effect a correction on the classical Volterra dislocation. The first order correction, the *dipolar moments*, has been the subject of investigation in the past by Clouet and collaborators [68,69] in the context of screw dislocations and was achieved by energetic methods [70]. Previous works [71–73] also attempted to model the core as a set of "line force" dipolar arrangements using atomistic calculation methods reliant on the core's energy.

In these works, a core energy is defined as the elastic energy that cannot be accounted for by the elastic energy of the Volterra dislocation. An ansatz is then made that the core's elastic field may be modeled by a set of equilibrated line forces in dipolar arrangements. This results in a set of dipoles of force, the moment tensor density of which is a symmetric dipolar tensor that serves to model the stress field of the dislocation core. In our case, the core field has originally been obtained from the considerations surrounding the core Kanzaki forces. These forces have been shown to not generally be in mechanical equilibrium. However, the elastic energy to harmonic order associated with core should be the same as that of Clouet's [68,69] and Hirth and coworkers' [71,72] accounts, since it comprises all non-Volterra effects too. Thus, contrary to these works, the dipolar and higher order multipolar moments we compute here do not necessitate that the core be in mechanical equilibrium; given that individual dislocations are known not to be in mechanical equilibrium [21,74,75], making such an assumption regardless will inevitably lead to a description of the core fields that is not comparable to the one discussed here. However, unlike in the case of Clouet [68,69] and Gehlen *et al.* [71], the multipolar terms introduced here do not account for all the core energy, which is only attained by considering the full multipolar expansion. The resulting dipolar and higher order multipolar fields introduced here serve to study with increasing accuracy the elastic near field of the dislocation core. However, for the reasons outlined above, they do not bear a one-to-one comparison with the alternative accounts produced by Clouet or Hirth and coworkers. In this work, the dipolar and higher order multipolar moment of arbitrary order follows directly from the Kanzaki force field alone, and no exploration of the core's energy landscape is necessary other than that leading to its structural minimization.

Formally, the nth-order multipolar moments of a force distribution $f_p(\mathbf{x})$ relative to some origin of coordinates are given by [76]

$$\gamma_{pk_1\ldots k_n}^{(n)} = \int_{\mathbb{R}^3} x_{k_1} \times \cdots \times x_{k_n} f_p(\mathbf{x}) d\mathbf{x}. \tag{26}$$

If, as is the case in a crystalline lattice, the forces are punctual and applied over specific perfect lattice positions $\mathbf{R} \equiv (l, k)$, then $f_p(\mathbf{x}) \equiv f_p(l, k)\delta(\mathbf{x} - \mathbf{R})$, whereupon

$$\gamma_{pk_1\ldots k_n}^{(n)} = \sum_{l,k} R_{k_1} \times \cdots \times R_{k_n} f_p(l, k). \tag{27}$$

The continuum level multipolar field expansion of $f_p(\mathbf{x})$ is then given by [76]

$$u_i(\mathbf{x}) = \sum_{n=0}^{\infty} \frac{(-1)^n}{n!} \frac{\partial^n G_{ip}(\mathbf{x})}{\partial x_{k_1} \dots \partial x_{k_n}} \gamma^{(n)}_{pk_1 \dots k_n}, \tag{28}$$

where $G_{ip}(\mathbf{x})$ is the elastic Green's function of the medium. The multipolar field expansion of $f_p(\mathbf{x})$ approximates to a very high degree of accuracy the long-range behavior of the elastic field generated by $f_p(\mathbf{x})$. This is because the elastic Green's function decays with $1/r$, so each of its subsequent derivatives will decay with an integer power of $1/r$ of increasing value [11]. Thus, the far field due to $f_p(\mathbf{x})$ is very well represented by the lowest order expansion terms [76].

Here, $f_p(\mathbf{x})$ is the Kanzaki force field. As was justified by Gurrutxaga-Lerma and Verschueren [21], the multipolar moments of the lattice can be employed in lieu of the whole Kanzaki force field to study the long-range behavior of their associated elastic field. However, a distinction needs to be made between the slip and core Kanzaki fields.

Indeed, as was shown in Ref. [21] for the case of screw dislocations, the multipolar expansion of the elastic fields of a defect is only available if the Kanzaki force field of the defect is compactly supported. This is because otherwise the central moments due to ever more remote point forces will be of increasing magnitude and lead to divergences when summed over. This entails that individual edge dislocations do not have a well-defined multipolar field because their slip Kanzaki force field extends to infinity, but clusters of edge dislocations where the slip surface is finite (e.g., a dipole of edge dislocations) do.

The core Kanzaki force field satisfies the compactness requirement for the existence of an associated multipolar field. The core's multipolar field expansion is therefore always possible, and offers a simple way of estimating its long range effects. The multipolar moments centered about the topological location of the dislocation line are given by

$$\gamma^{\text{core}}_{pk_1 \dots k_n} = \sum_{l,k} R_{k_1} \times \dots \times R_{k_n} f^{\text{core}}_p(l,k). \tag{29}$$

The core multipolar moments associated with the force fields given in Fig. 5 are collected in Table I. The effect of these corrections is discussed in the following sections.

D. Energetic considerations

As stated in Sec. II and in the Supplemental Material, the energy of the Kanzaki force field is that of the defect in the harmonic approximation. The energy associated with the core Kanzaki field is (excluding anharmonicities):

$$V^{\text{core}} = V^K - V^{\text{slip}} \tag{30}$$

where V^K is the full dislocation's energy in the harmonic approximation, and V^{slip} the Volterra dislocation's energy in the harmonic approximation. Both have well-defined forms: V^K is given by Eq. (17) in the Supplemental Material, and similarly

$$\begin{aligned} V^{\text{slip}} &= \sum_{l,k} f^{\text{slip}}_i(l,k) u^{\text{Volterra}}_i(l,k) \\ &= \sum_{(l,k),(l',k')} \Phi_{ij}(l-l',k-k') B_i B_j \chi^2_S(l-l',k-k'), \end{aligned} \tag{31}$$

where $\chi^2_S(l-l',k-k') = 1$ if the bond (l,k)-(l',k') crosses the slip surface and 0 otherwise.

As a result, the core energy is affected by the slip Kanzaki field:

$$\begin{aligned} V^{\text{core}} &= \sum_{l,k} \left[f^K_i(l,k) u_i(l,k) - f^{\text{slip}}_i(l,k) u^{\text{Volterra}}_i(l,k) \right] \\ &= \sum_{l,k} \left[f^K_i(l,k) + f^{\text{slip}}_i(l,k) \right] u^{\text{Volterra}}_i(l,k) \quad \text{or} \\ &= \sum_{l,k} f^{\text{core}}_i(l,k) \left[u^K_i(l,k) + u^{\text{Volterra}}_i(l,k) \right]. \end{aligned} \tag{32}$$

According to this definition, the total core energy will grow with the dislocation line's length. We may average it over unit cell sizes in line's direction to obtain a *dislocation line energy* $\langle V^{\text{core}} \rangle = V^{\text{core}}/\delta z$, where δz is a unit cell width in the dislocation line's direction. We find that over a few unit cell distances, the core's line energy $\langle V^{\text{core}} \rangle$ converges to a given value; Fig. 8 shows this convergence for the case of fcc Al.

The definition of a core energy given by Eq. (32) is notionally analogous to the classical definition of the core energy (see Refs. [27,44,77]). The line energy of a dislocation is divided into two superposed terms: an elastic term associated with the Volterra dislocation's energy and a core energy term that accounts for the differences between the total and elastic

TABLE I. Computed values for the core multipolar moments for the dipole and quadrupole core corrections. Note that their relative symmetry is reliant on whether the core field is in mechanical equilibrium, which need not be the case.

Core multipolar moments	Al	Ta	Cu	W
γ_{11} (eV)	−7.22	30.61	−27.61	−56.35
γ_{12} (eV)	−4.29	−4.67	−31.47	20.05
γ_{21} (eV)	−4.28	3.68	50.43	20
γ_{22} (eV)	−10.33	−1.65	−35.27	−9.63
γ_{31} (eV)	−1.435	0	−49.1	−21.06
γ_{32} (eV)	−6.83	0	−1.572	3.04
γ_{111} (eV Å)	−19.65	897.01	−331.23	−839.5
γ_{112} (eV Å)	−57.98	−237.22	250.72	−73.5
γ_{122} (eV Å)	−0.14	9.92	277.52	−118.46
γ_{211} (eV Å)	−111.55	−79.9	760.1	−118.45
γ_{212} (eV Å)	−62.3	−24.24	−490.03	−22.48
γ_{222} (eV Å)	2.56	7.49	−1785.41	12.74
γ_{311} (eV Å)	−20.3	0	885.83	56.65
γ_{312} (eV Å)	−13.01	0	−93.04	156.65
γ_{322} (eV Å)	−2.14	0	−852.39	56.65

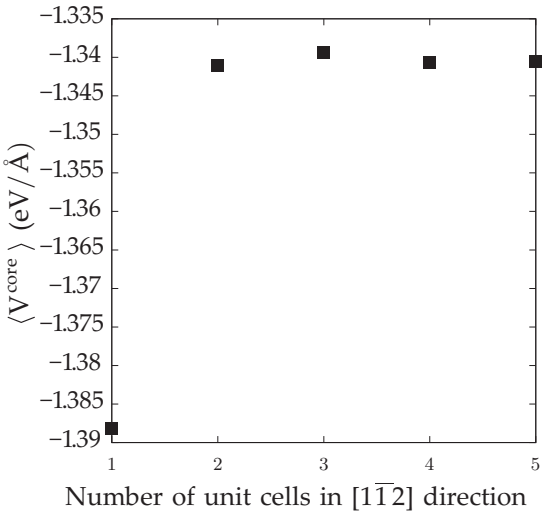

FIG. 8. Average core energy for fcc Al.

terms. Typically the elastic energy takes the form [27]

$$E_{\text{core}} = \frac{\mu B^2}{4\pi(1-\nu)} \ln \frac{r_0}{r}, \tag{33}$$

where r is the radial distance to the nominal dislocation line, and r_0 is the *core radius*; hereafter, the letter E is employed to distinguish the energy coming from continuum level considerations from the energy V coming from lattice level models. The core radius is defined as the radial distance above which the elastic fields of the dislocation satisfy linear elasticity [77]. This makes the core radius an ambiguously defined variable [78], with the value of the core energy heavily dependent on both its value and the assumption that the dislocation and its core are planar (cf. Ref. [27]).

The Kanzaki force field approach provides us with an alternative, less ambiguous definition of the core's energy because neither the core radius nor the planarity of the core are necessary hypotheses to define it. As may be seen in Eq. (32), there is no need for a core radius because the elastic part of the line energy [in this case, the V^{slip} in Eq. (31)] is extended to the dislocation line itself: It sums over, atom by atom, the product of the $B_i\chi_S(l-l',k-k')$ slip distribution with the associated slip Kanzaki force field (represented in Fig. 4) as expected. This quantity is nondivergent because both the forces and displacements have well-defined values and because it does not depend on linear elastic assumptions: V^{slip} is given a well-defined atomistic value. Arguably, Eq. (31) could be taken to the long wave limit, which recovers the classical definition of the elastic energy of a Volterra dislocation. Indeed, in the long wave limit, and neglecting all core Kanzaki forces, $f_x^{BK}(x,y) = B\mu H(x)\delta'(y)$, $f_y^{BK} = B\mu\delta(x)\delta(y)$, $u_x(x,y) = B/(2\pi)\{\arctan(y/x)+1/[2(1-\nu)]xy/r^2\}$, $u_y(x,y)=B/(2\pi)\{(1-2\nu)/[2(1-\nu)]\ln(1/r)+1/[2(1-\nu)]y^2/r^2\}$, and with appropriately bound limits

$$E_{\text{elastic}} = \int_{\mathbb{R}^2} f_i^{BK} u_i dxdy = \frac{\mu B^2}{4\pi(1-\nu)} \ln \frac{r}{r_0}. \tag{34}$$

Given that using our approach both the slip and the full Kanzaki forces (and the associated affine maps) are available in the atomistic system, the definition of the core energy in Eq. (32) allows us to offer an unambiguous account of how much configurational energy is due to the presence of a non-Volterra dislocation core as opposed to a perfect Volterra dislocation. More specifically, the core energy definition provided accounts for the energy involved in relaxing the atomic positions from a pure Volterra configuration to the minimized configuration.

Accordingly, the values of the core energy we find, although within the same order of magnitude as those commonly reported (see Refs. [77,78]), will nonetheless be different. For instance, we find that for fcc Al, over a few unit cells the $\langle V^{\text{core}}\rangle$ converges to a value of about $\langle V^{\text{core}}\rangle_{\text{Al}} = -1.34\,\text{eV/Å}$. For comparison's sake, the core energy estimated using the classical elastic definition of Eq. (34) for Al is $E_{\text{core}} = 0.42\,\text{eV/Å}$ for $r_0 = 10\,$Å, which is close to previously reported values [77]. As is shown in the Supplemental Material, the relationship between the core energy and the multipolar fields is not immediate.

E. Example: Elastic field of the fcc Cu edge dislocation

The procedure for obtaining an elastic model of a dislocation based on the Kanzaki force field may be summarized as follows:

(1) A sufficiently large perfect crystal Ω_0 is defined.

(2) A dipole of edge dislocations is introduced into the crystal by producing a crystallographic slip of $\pm B/2$ across the nominal slip surface.

(3) The system is minimized so as to obtain the relaxed structure, Ω_d.

(4) The affine mapping $\mathbf{u}(l,k)$ is computed by comparing Ω_0 and Ω_d.

(5) The Kanzaki force field $f_i^K(l,k)$ is computed by multiplying the affine mapping $\mathbf{u}(l,k)$ with Ω_0 (the perfect lattice's) force constant matrix, $\Phi_{ij}(l-l',k-k')$.

(6) The slip Kanzaki force field, $f_i^{\text{slip}}(l,k)$, is computed by multiplying the Volterra displacement $u_i^{\text{slip}} = B_i\chi_s(l-l',k-k')$ with Ω_0 (the perfect lattice's) force constant matrix, $\Phi_{ij}(l-l',k-k')$.

(7) Compute the core Kanzaki force field as $f_i^{\text{core}}(l,k) = f_i^K(l,k) - f_i^{\text{slip}}(l,k)$.

(8) Construct the core's elastic fields by multiplying the $f_i^{\text{core}}(\mathbf{x})G_{ij}(\mathbf{x})$ and summing over the Volterra dislocation's fields.

Here, owing to the particularly wide dislocation core, focus is placed on the edge dislocation in fcc Cu—the other metals' dislocations can be obtained by analogous means, and their respective field models are reproduced in the Supplemental Material. Figure 9 represents the three in-plane components of the stress field of the fcc Cu edge dislocation and compares their shape and magnitude with the corresponding atomistic stress fields. Good agreement is observed. These "corrected" field components are obtained by superposition of the Volterra dislocation's fields with the core Kanzaki forces, **defined via Eq. (11). As can be seen**, the principal features of the dissociated core

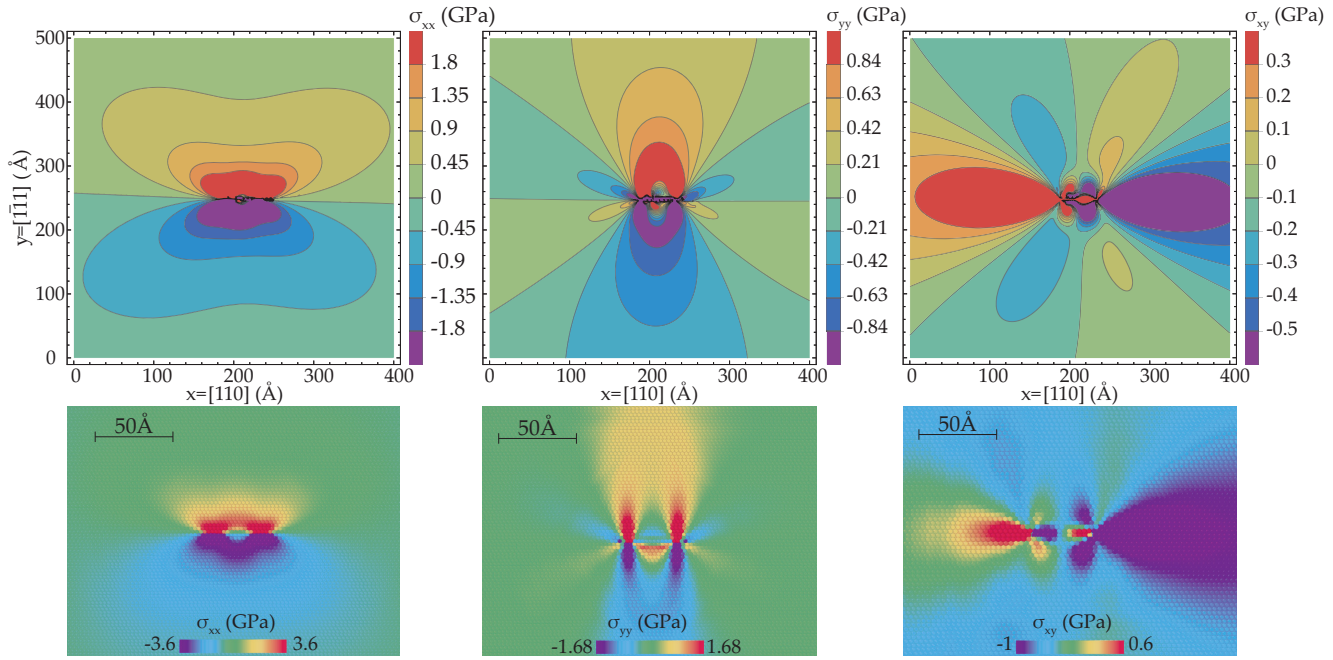

FIG. 9. In-plane stress field components of the elastic model of an edge dislocation in fcc Cu using the Kanzaki core field alongside the Volterra contribution. The fields are compared to the atomistic stress field components, showing good agreement.

are adequately captured by the elastic field implied by the Kanzaki force field. The deviation from the Volterra dislocation's stress fields is notable particularly in the short range, where the core width is significant enough to entail considerable variations in the dislocation's short-range interactions with other dislocations or defects.

Figure 10 shows the antiplanar effects that the Kanzaki force field of the dislocation enable capturing. These antiplanar components are not present in the classical Volterra edge dislocation and arise due to the stacking fault at the core of the dislocation. As has been shown in Fig. 7(b), these entail a set of f_z antiplanar Kanzaki forces localized around the core, which results in the stress fields shown in Fig. 10. These stress fields are entirely localized about the dislocation core but of noticeable magnitude. Their long-range effects may be estimated via the dipolar moments associated with these stress field components (collected in Table I). In either case, $\sigma_{3i} \propto \gamma_{31}, \gamma_{32}$. Thus, for σ_{32}, for example, we have

$$\sigma_{32} \equiv \sigma_{zy} \approx \frac{2\gamma_{31}xy + \gamma_{32}(y^2 - x^2)}{4\pi(x^2 + y^2)^2}. \tag{35}$$

In this case, $\gamma_{31} = -49.1$ eV, $\gamma_{32} = 1.572$ eV. This is entirely consistent with the computed Kanzaki core field and the physical nature of the core: The core is largely extended along the $x = [1\,1\,0]$ but remains very narrowly localized along the $y = [\bar{1}\,1\,1]$ direction, so accordingly the core's antiplanar dipolar moment along x, γ_{31}, is bound to be large, while the dipolar moment γ_{32} along y ought to be very small. In accordance, the long-range effect of the core's antiplane component will be dominated by γ_{31} and decay as

$$\sigma_{31}, \sigma_{32} \propto \frac{\gamma_{31}}{r}. \tag{36}$$

The γ_{31} dipolar moment is of the same magnitude as the core's in-plane dipolar moments [$\approx$ O(10)eV; see Table I], which signifies that all core contributions, which act superposed to the Volterra dislocation's fields, are expected to decay with the same speed and be of similar magnitude to one another. In particular, this means that $\approx$10B distances away from the core will be of the order of several hundreds of MPa stronger than predicted by the classical Volterra solution. This long-range intensity of the core itself can be shown to have strong effects on the mid- to short-range interactions between dislocations. Figure 11 compares the long-range differences in σ_{12} (i.e., the resolved shear stress acting on the slip plane, with which another dislocation on the same slip place would interact) between the Volterra dislocation, the edge dislocation represented by the Kanzaki force field, and the Volterra dislocation corrected with the core's dipolar fields. As can be seen, the Volterra dislocation underestimates the σ_{12} stress field intensity; the dipolar correction improves on it in the long-range, but it remains insufficient to adequately captured the predicted intensity of the shear stress field. Beyond the distances shown in Fig. 11, (i.e., for distances of the order of or longer than $\approx$100 nm), the Volterra dislocation remains an accurate representation of the dislocation's long-range effects, so core effects remain important only for short-range interactions.

Similar remarks may be made about the edge dislocations of the different metals discussed in this work. In all these cases, summarized in Figs. 2, 3, and 4 of the Supplemental Material, the Kanzaki force field enables a detailed study of the deviations caused by the non-Volterra core on the short- and long-range interactions of the dislocation. Depending on factors including the core's width—which is generally small in bcc metals and for high stacking fault fcc metals—or the slip plane's curvature—which as has been discussed is

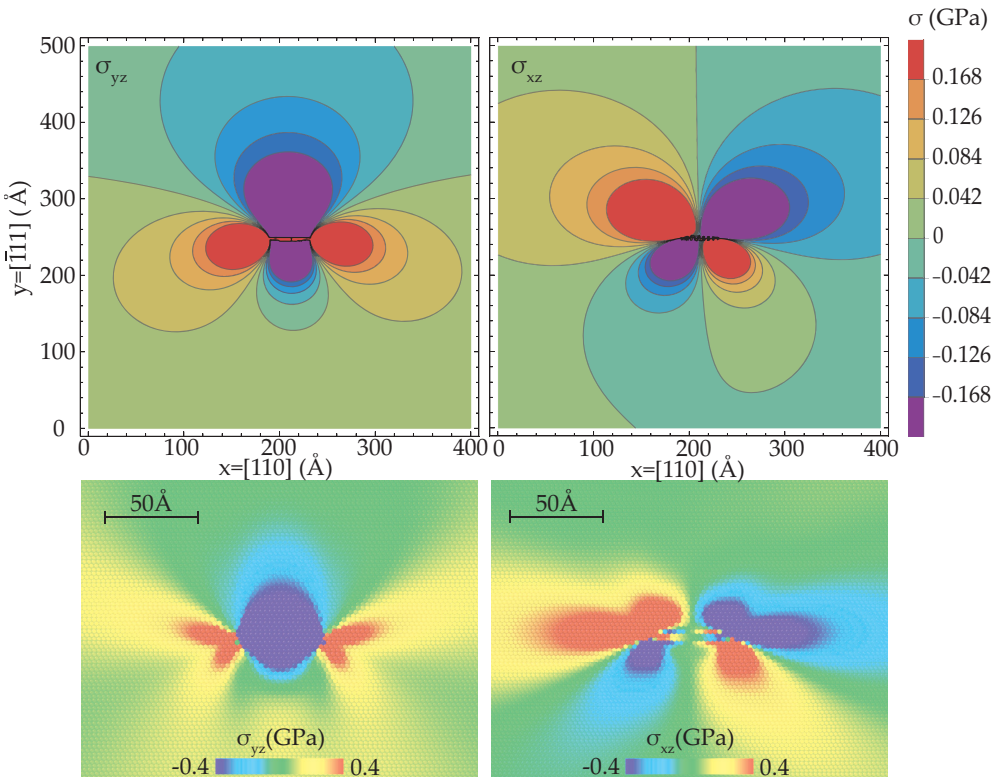

FIG. 10. Antiplanar stress field components of the elastic model of an edge dislocation in fcc Cu using the Kanzaki core field. There is no antiplanar Volterra contribution to the stress field components [27].

noticeable for the ⟨111⟩{112} edge dislocation in Ta—the dislocation's Kanzaki force field will impart noticeable differences in the short- to midrange interactions of the dislocation. Crucially, the Kanzaki force field facilitates a one-to-one map between the atomistic crystalline lattice and the defect's continuum level model. In the case of edge dislocations, it provides an entirely three-dimensional model of the dislocation and its core, and it enables capturing core effects that are usually missed in other dislocation core models such as the Peierls-Nabarro model [27]; whereas the latter is dependent on the *ad hoc* assumption that the core is planar and mollifies the slip distribution according to physical considerations concerning the Peierls barrier and the γ surface (see Refs. [27,79]), the Kanzaki force field is a mechanistic expression of the forces that would have to be applied on the atoms to generate the global topology of the defect. As such, they facilitate a more complete description of the core's geometry and long-range fields. However, they do not necessarily regularize the core unless the underlying continuum level theory of elasticity employed alongside them enables to do so: In the current work, first-order linear elasticity has been employed, but alternatively a nonlocal [80] or gradient elasticity theories [81–83] could have been employed, in which case the elastic field models extracted from the Kanzaki force field would be regularized by construction (cf. Refs. [82,83]).

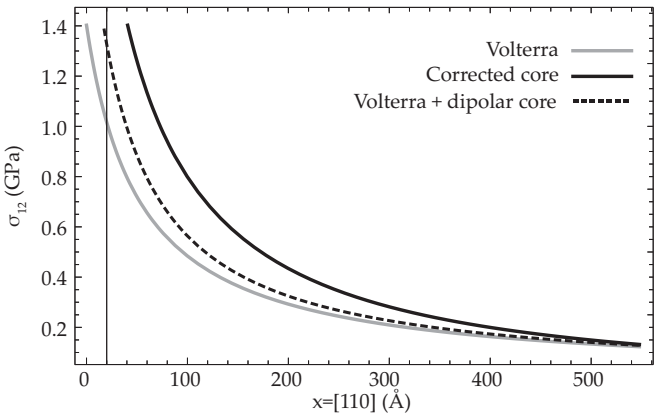

FIG. 11. Comparison of the magnitude of the σ_{12} stress field component acting on the slip plane's direction for a Volterra edge dislocation in fcc Cu, the fully corrected dislocation where the core fields are represented with the core Kanzaki force field shown in Fig. 5(c), and the Volterra dislocation corrected with the core's dipolar field. The vertical line indicates the approximate location of the first dislocation partial; the core is located at −15 Å.

VI. CONCLUSIONS

This article has developed a general procedure for computing the Kanzaki force field of a general extended defect. The Kanzaki force field has been defined as the set of forces that would have to be applied in a perfect harmonic lattice to generate the topology of the said defect. The topology of the defect is defined in terms of an affine mapping between the positions of the atoms in the perfect lattice and the positions of the atoms in the relaxed, defective lattice; the affine mapping is necessary to ensure that the harmonic approximation can

be applied to each atom in the defective lattice. The Kanzaki force field is then obtained as the product of this mapping with the perfect lattice's force constant matrix. This article has shown that (a) the Kanzaki force field generates the topology of the defect in a harmonic lattice, (b) the Kanzaki force field converges to the linear elastic Burridge-Knopoff force representation of the defect in the long wave limit, and (c) the energy associated with the Kanzaki force field is the energy of the defect in the harmonic approximation. These results lead us to conclude Kanzaki force field can be employed as source terms of the elastic fields of the defect both in lattice statics and dynamics and in the elastic continuum. The continuum level models are geometrically true to the topology of the defect, and the associated elastic fields are an accurate representation of the defects.

Given that the affine mapping may be defined for any extended defect, the Kanzaki force field methodology described in this work can be employed to model general extended defects with the expectation of producing atomistically informed models that are geometrically and energetically accurate. These could be employed in producing atomistically informed models of dislocations, twin and grain boundaries, or cracks, among other extended defects.

As means of an example, in this article particular focus has been placed on the modeling of edge dislocations in a number of cubic metals. The affine mappings for edge dislocations in fcc Al, fcc Cu, bcc W, and bcc Ta, obtained from energy minimizations using appropriate phenomenological interatomic potentials, have been employed to compute their corresponding Kanzaki fore field. It has been shown that the Kanzaki force field of edge dislocations consists of two distinct contributions: (1) a *Volterra* contribution associated with the slip or disregistry acting across the nominal slip surface, which characterizes the classical Volterra dislocation, and (2) a *core* distribution associated with the dislocation's core specific topology.

As has been discussed, the Volterra field agrees with the continuum level force representation of a dislocation based on the Burridge-Knopoff theorem. The core Kanzaki field accounts for the deviations away from the Volterra disregistry. This mostly concerns the atoms about the dislocation core—away from it, the computed Kanzaki force field is always Volterra. As has been shown, the core Kanzaki field is entirely three dimensional, generally entailing both in-plane and antiplane force components. This provides a tool for studying the nonplanarity of the core of dislocations and their effects in short-range interactions with other dislocations or defects. Here, we have found that the core of edge dislocations in fcc metals is bound to be nonplanar, owing to the antiplanar Kanzaki forces associated with the intrinsic stacking fault lying at the core. For bcc metals, the core may or may not be perfectly planar depending on the specific crystallographic orientation of the dislocation.

Thus, when applied to the study of dislocations the Kanzaki force field has been shown to produce a one-to-one map of the dislocations core's specific geometry, capturing both planar and antiplanar effects. Furthermore, the Kanzaki force field offers an unambiguous definition of the core energy of the dislocation. This is because the Kanzaki force field allows for a clear-cut distinction between the forces necessary to generate a perfect unitary disregistry across the slip surface—which in the long wave limit becomes the classical Volterra dislocation—and the forces necessary to thereafter displace the atoms to the final, relaxed positions that define the actual dislocation. The work involved in driving the perfect lattice to the Volterra and relaxed positions (which is exerted by the Kanzaki forces), defines both the slip energy and core energy of the dislocation in an univocal way, and the resulting line energies do not necessitate a core radius to remain finite.

Core and other local effects can be studied via the multipolar moments of the core, which have been defined in this work and can in general be simply obtained by computing the Kanzaki force field's actual vectorial moments. These moments enable the obtention of successively more accurate descriptions of the near field about the core and provide the basis for an estimate of short-range effects in the three spatial directions. As has been found, these are generally weaker than the dislocation's Volterra fields. Their relationship to the core energy via the core's distortion tensor has been discussed as well.

In summary, the generalized Kanzaki force field has been shown to offer a uniquely accurate tool to mode crystalline defects in lattice statics and in the continuum. The method enables the direct multiscale transfer of information regarding the topology and energetics of the defect from atomistic systems to the continuum. This is facilitated because linear elasticity is a specific limit of the harmonic lattice. With the use of adequate atomistic tools, the Kanzaki force field approach avoids the need for more continuum level phenomenological descriptions of the near field of dislocations such as the Peierls-Nabarro model. In particular, it would enable more accurate models of interactions between dislocations and point defects [84], facilitate the transfer of information between concurrent multiscale models [85,86] of molecular dynamics schemes and dislocation dynamics simulations of solids [87,88], and enable the creation of more accurate models for damage under lattice irradiation [14,89], explicit continuum level models of extended defects such as crowdions [14,90], and low-angle grain boundaries or twin boundaries [91], among many other potential applications. Furthermore, the Kanzaki force field provides a lattice description of the defect; this may be employed in studying the mobility of defects such as dislocations using lattice dynamics [26].

ACKNOWLEDGMENTS

B.G.-L. gratefully acknowledges the munificent support of the Master and Fellows of Trinity College Cambridge under the author's Title A Fellowship. J.V. was supported through a studentship in the Centre for Doctoral Training on Theory and Simulation of Materials at Imperial College London funded by EPSRC under Grant No. EP/L015579/1.

[1] H. Kanzaki, Point defects in face-centred cubic lattice—I. Distortion around defects, J. Phys. Chem. Solids **2**, 24 (1957).

[2] H. Kanzaki, Point defects in face-centred cubic lattice—II. X-ray scattering effects, J. Phys. Chem. Solids **2**, 107 (1957).

[3] H. R. Schober and K. W. Ingle, Calculation of relaxation volumes, dipole tensors, and Kanzaki forces for point defects, J. Phys. F **10**, 575 (1980).
[4] J. S. Galsin, *Impurity Scattering in Metallic Alloys* (Springer, Berlin, 2012).
[5] M. J. Gillan, The elastic dipole tensor for point defects in ionic crystals, J. Phys. C: Solid State Phys. **17**, 1473 (1984).
[6] C. Varvenne and E. Clouet, Elastic dipoles of point defects from atomistic simulations, Phys. Rev. B **96**, 224103 (2017).
[7] J. R. Hardy and R. Bullough, Point defect interactions in harmonic cubic lattices, Philos. Mag. **15**, 237 (1967).
[8] J. M. Harder and D. J. Bacon, Point-defect and stacking-fault properties in body-centred-cubic metals with *n*-body interatomic potentials, Philos. Mag. A **54**, 651 (1986).
[9] P. H. Dederichs, C. Lehmann, H. R. Schober, A. Scholz, and R. Zeller, Lattice theory of point defects, J. Nucl. Mater. **69**, 176 (1978).
[10] E. J. Savino, Point defect-dislocation interaction in a crystal under tension, Philos. Mag. **36**, 323 (1977).
[11] R. W. Balluffi, *Introduction to Elasticity Theory for Crystal Defects* (World Scientific, Singapore, 2017).
[12] G. Simonelli, R. Pasianot, and E. J. Savino, Point-defect computer simulation including angular forces in bcc iron, Phys. Rev. B **50**, 727 (1994).
[13] C. Freysoldt, B. Grabowski, T. Hickel, J. Neugebauer, G. Kresse, A. Janotti, and C. G. Van de Walle, First-principles calculations for point defects in solids, Rev. Mod. Phys. **86**, 253 (2014).
[14] S. L. Dudarev and P.-W. Ma, Elastic fields, dipole tensors, and interaction between self-interstitial atom defects in bcc transition metals, Phys. Rev. Mater. **2**, 033602 (2018).
[15] P.-W. Ma and S. L. Dudarev, Universality of point defect structure in body-centered cubic metals, Phys. Rev. Mater. **3**, 013605 (2019).
[16] E. Hayward, C. Deo, B. P. Uberuaga, and C. N. Tomé, The interaction of a screw dislocation with point defects in bcc iron, Philos. Mag. **92**, 2759 (2012).
[17] H. Dosch, A. V. Schwerin, and J. Peisl, Point-defect-induced nucleation of the ω phase, Phys. Rev. B **34**, 1654 (1986).
[18] R. Nazarov, J. S. Majevadia, M. Patel, M. R. Wenman, D. S. Balint, J. Neugebauer, and A. P. Sutton, First-principles calculation of the elastic dipole tensor of a point defect: Application to hydrogen in α-zirconium, Phys. Rev. B **94**, 241112 (2016).
[19] R. Pawellek, M. Fahnle, C. Elsasser, K.-M. Ho, and C.-T. Chan, First-principles calculation of the relaxation around a vacancy and the vacancy formation energy in bcc Li, J. Phys.: Condens. Matter **3**, 2451 (1991).
[20] B. Yang and V. K. Tewary, Multiscale modeling of point defects in Si-Ge (001) quantum wells, Phys. Rev. B **75**, 144103 (2007).
[21] B. Gurrutxaga-Lerma and J. Verschueren, Elastic models of dislocations based on atomistic Kanzaki forces, Phys. Rev. B **98**, 134104 (2018).
[22] S. Ishioka, Uniform motion of a screw dislocation in a lattice, J. Phys. Soc. Jpn. **30**, 323 (1971).
[23] V. Celli and N. Flytzanis, Motion of a screw dislocation in a crystal, J. Appl. Phys. **41**, 4443 (1970).
[24] L. L. Boyer and J. R. Hardy, Lattice statics applied to screw dislocations in cubic metals, Philos. Mag. **24**, 647 (1971).
[25] J. A. Caro and N. Glass, A lattice-dynamics model of the interaction of a dislocation with point defects, J. Phys. **45**, 1337 (1984).
[26] J. Verschueren, B. Gurrutxaga-Lerma, D. S. Balint, A. P. Sutton, and D. Dini, Instabilities of High-Speed Dislocations, Phys. Rev. Lett. **121**, 145502 (2018).
[27] J. P. Hirth and J. Lothe, *Theory of Dislocations*, 2nd ed. (Wiley, New York, 1982).
[28] P. B. Hirsch, A. Howie, R. Nicholson, D. W. Pashley, and M. J. Whelan, *Electron Microscopy of Thin Crystals* (Butterworths, London, 1974).
[29] R. Burridge and L. Knopoff, Body force equivalents for seismic dislocations, Bull. Seismol. Soc. Am. **54**, 1875 (1964).
[30] G. Backus and M. Mulcahy, Moment tensors and other phenomenological descriptions of seismic sources—I. Continuous displacements, Geophys. J. Int. **46**, 341 (1976).
[31] G. Backus and M. Mulcahy, Moment tensors and other phenomenological descriptions of seismic sources—II. Discontinuous displacements, Geophys. J. Int. **47**, 301 (1976).
[32] E. Van der Giessen and A. Needleman, Discrete dislocation plasticity: A simple planar model, Model. Simul. Mater. Sci. Eng. **3**, 689 (1995).
[33] I. Vaisman, *Analytical Geometry* (World Scientific, Singapore, 1997), Vol. 8.
[34] N. W. Ashcroft and N. D. Mermin, *Solid State Physics* (Brooks/Cole, Belmont, MA, 1976).
[35] M. Born and K. Huang, *Dynamical Theory of Crystal Lattices* (Oxford University Press, New York, 1998).
[36] See Supplemental Material at http://link.aps.org/supplemental/10.1103/PhysRevMaterials.3.113801 for a description of the relationship between the Kanzki force representation and the Burridge-Knopoff forces, a proof that the Kanzaki forces act as source terms in the harmonic lattice and the continuum, several energetic considerations regarding the Kanzaki force representation, a numerical verification that their magnitude agrees with the predicted BK forces, and the stress field components for fcc Al, bcc W, and bcc Ta.
[37] R. M. Martin, *Electronic Structure: Basic Theory and Practical Methods* (Cambridge University Press, Cambridge, UK, 2004).
[38] D. Frenkel and B. Smit, *Understanding Molecular Simulations: From Algorithms to Applications* (Elsevier, Amsterdam, 2001).
[39] P. Varotsos and K. Alexopoulos, Calculation of the formation entropy of vacancies due to anharmonic effects, Phys. Rev. B **15**, 4111 (1977).
[40] J. D. Clayton and D. J. Bammann, Finite deformations and internal forces in elastic-plastic crystals: Interpretations from nonlinear elasticity and anharmonic lattice statics, J. Eng. Mater. Technol. **131**, 041201 (2009).
[41] C. Teodosiu, *Elastic Models of Crystal Defects* (Springer-Verlag, London, 1982).
[42] E. Kröner, *Kontinuumstheorie der Vemetrungen und Eigenspannungen*, Vol. 5 of *Ergebnisse der Angewandten Mathematik* (Springer-Verlag, Berlin, 1958).
[43] E. Kröner and B. K. Datta, Non-local theory of elasticity for a finite inhomogeneous medium: A derivation from lattice theory, in *Fundamental Aspects of Dislocation Theory, Conference Proceedings*, Vol. 2, edited by J. A. Simmons, R. deWit, and R. Bullough (Institute of Materials Research, National Bureau of Standards, Washington, DC, 1969), pp. 737–746.

[44] D. Hull and D. J. Bacon, *Introduction to Dislocations*, 5th ed. (Butterworth-Heinemann, Oxford, UK, 2011).

[45] K. B. Broberg, *Cracks and Fracture* (Academic Press, New York, 1999).

[46] A. P. Sutton and R. W. Balluffi, *Interfaces in Crystalline Materials* (Oxford University Press, Oxford, UK, 2006).

[47] V. Vitek, Structure of dislocation cores in metallic materials and its impact on their plastic behaviour, Prog. Mater. Sci. **36**, 1 (1992).

[48] K. Ito and V. Vitek, Atomistic study of non-Schmid effects in the plastic yielding of bcc metals, Philos. Mag. A **45**, 1387 (2001).

[49] M. S. Duesbery, V. Vitek, and D. K. Bowen, The effect of shear stress on the screw dislocation core structure in body-centred cubic lattices, Proc. R. Soc. London A **332**, 85 (1973).

[50] J. A. Moriarty, V. Vitek, V. V. Bulatov, and S. Yip, Atomistic simulations of dislocations and defects, J. Comput.-Aided Mater. Des. **9**, 99 (2002).

[51] S. Plimpton, P. Crozier, and A. Thompson, Lammps-large-scale atomic/molecular massively parallel simulator, Tech. Rep. 18:43, Sandia National Laboratories, 2007 (unpublished).

[52] T. H. Cormen, C. E. Leiserson, T. L. Rivest, and C. Stein, *Introduction to Algorithms* (MIT Press, Cambridge, MA, 2009).

[53] J. L. Blanco and P. K. Rai, nanoflann: a C++ header-only fork of FLANN, a library for nearest neighbor (NN) with kd-trees, https://github.com/jlblancoc/nanoflann.

[54] M. S. Daw and M. I. Baskes, Embedded-atom method: Derivation and application to impurities, surfaces, and other defects in metals, Phys. Rev. B **29**, 6443 (1984).

[55] G. J. Ackland, G. Tichy, V. Vitek, and M. W. Finnis, Simple *n*-body potentials for the noble metals and nickel, Philos. Mag. A **56**, 735 (1987).

[56] X.-Y. Liu, F. Ercolessi, and J. B. Adams, Aluminium interatomic potential from density functional theory calculations with improved stacking fault energy, Model. Simul. Mater. Sci. Eng. **12**, 665 (2004).

[57] R. Ravelo, T. C. Germann, O. Guerrero, Q. An, and B. L. Holian, Shock-induced plasticity in tantalum single crystals: Interatomic potentials and large-scale molecular-dynamics simulations, Phys. Rev. B **88**, 134101 (2013).

[58] S. Han, L. A. Zepeda-Ruiz, G. J. Ackland, R. Car, and D. J. Srolovitz, Interatomic potential for vanadium suitable for radiation damage simulations, J. Appl. Phys. **93**, 3328 (2003).

[59] A. Stukowski, V. V. Bulatov, and A. Arsenlis, Automated identification and indexing of dislocations in crystal interfaces, Model. Simul. Mater. Sci. Eng. **20**, 085007 (2012).

[60] A. Stukowski, Visualization and analysis of atomistic simulation data with Ovito—the open visualization tool, Model. Simul. Mater. Sci. Eng. **18**, 015012 (2009).

[61] E. B. Tadmor and R. E. Miller, *Modeling Materials: Continuum, Atomistic, and Multiscale Techniques* (Cambridge University Press, Cambridge, UK, 2011).

[62] B. Jacob, G. Guennebaud *et al.*, Eigen: C++ template library for linear algebra, 2013, http://eigen.tuxfamily.org.

[63] Y. Mishin, Interatomic potentials for metals, in *Handbook of Materials Modeling* (Springer, Berlin, 2005), pp. 459–478.

[64] C. Campaná and M. H. Müser, Practical Green's function approach to the simulation of elastic semi-infinite solids, Phys. Rev. B **74**, 075420 (2006).

[65] J. Cho, J.-F. Molinari, W. A. Curtin, and G. Anciaux, The coupled atomistic/discrete-dislocation method in 3d. Part III: Dynamics of hybrid dislocations, J. Mech. Phys. Solids **118**, 1 (2018).

[66] K. Aki and P. G. Richards, *Quantitative Seismology*, 2nd ed. (University Science Books, Sausalito, CA, 2002).

[67] T. Mura, *Micromechics of Defects in Solids*, 2nd ed. (Kluwer Academic, Amsterdam, 1982).

[68] E. Clouet, Dislocation core field. I. Modeling in anisotropic linear elasticity theory, Phys. Rev. B **84**, 224111 (2011).

[69] E. Clouet, L. Ventelon, and F. Willaime, Dislocation core field. II. Screw dislocation in iron, Phys. Rev. B **84**, 224107 (2011).

[70] E. Clouet, L. Ventelon, and F. Willaime, Dislocation Core Energies and Core Fields from First Principles, Phys. Rev. Lett. **102**, 055502 (2009).

[71] P. C. Gehlen, J. P. Hirth, R. G. Hoagland, and M. F. Kanninen, A new representation of the strain field associated with the cube-edge dislocation in a model of a α-iron, J. Appl. Phys. **43**, 3921 (1972).

[72] J. P. Hirth and J. Lothe, Anisotropic elastic solutions for line defects in high-symmetry cases, J. App. Phys. **44**, 1029 (1973).

[73] J. E. Sinclair, P. C. Gehlen, R. G. Hoagland, and J. P. Hirth, Flexible boundary conditions and nonlinear geometric effects in atomic dislocation modeling, J. Appl. Phys. **49**, 3890 (1978).

[74] U. F. Kocks and R. O. Scattergood, Elastic interactions between dislocations in a finite body, Acta Metall. **17**, 1161 (1969).

[75] Mechanical equilibrium can only be achieved if the slip surface is finite [21].

[76] B. Gurrutxaga-Lerma, Static and dynamic multipolar field expansions of dislocations and cracks in solids, Int. J. Eng. Sci. **128**, 165 (2018).

[77] X. W. Zhou, R. B. Sills, D. K. Ward, and R. A. Karnesky, Atomistic calculations of dislocation core energy in aluminium, Phys. Rev. B **95**, 054112 (2017).

[78] G. Lu, N. Kioussis, V. V. Bulatov, and E. Kaxiras, Generalized-stacking-fault energy surface and dislocation properties of aluminum, Phys. Rev. B **62**, 3099 (2000).

[79] M. Boleininger, T. D. Swinburne, and S. L. Dudarev, Atomistic-to-continuum description of edge dislocation core: Unification of the Peierls-Nabarro model with linear elasticity, Phys. Rev. Mater. **2**, 083803 (2018).

[80] E. Kröner, Interrelations between various branches of continuum mechanics, in *Mechanics of Generalized Continua* (Springer, Berlin, 1968), pp. 330–341.

[81] B. S. Altan and E. C. Aifantis, On some aspects in the special theory of gradient elasticity, J. Mech. Behav. Mater. **8**, 231 (1997).

[82] M. Y. Gutkin and E. C. Aifantis, Dislocations and disclinations in gradient elasticity, Phys. Status Solidi B **214**, 245 (1999).

[83] J. Kioseoglou, G. P. Dimitrakopulos, Ph. Komninou, Th. Karakostas, I. Konstantopoulos, M. Avlonitis, and E. C. Aifantis, Analysis of partial dislocations in wurtzite GaN using gradient elasticity, Phys. Status Solidi A **203**, 2161 (2006).

[84] E. Clouet, S. Garruchet, H. Nguyen, M. Perez, and C. S. Becquart, Dislocation interaction with C in α-Fe: A comparison between atomic simulations and elasticity theory, Acta Mater. **56**, 3450 (2008).

[85] J. Fish, M. A. Nuggehally, M. S. Shephard, C. R. Picu, S. Badia, M. L. Parks, and M. Gunzburger, Concurrent ATC coupling based on a blend of the continuum stress and the atomistic force, Comput. Methods Appl. Mech. Eng. **196**, 4548 (2007).

[86] S. Badia, M. L. Parks, P. Bochev, M. Gunzburger, and R. Lehoucq, On atomistic-to-continuum coupling by blending, Multiscale Model. Simul. **7**, 381 (2008).

[87] L. E. Shilkrot, R. E. Miller, and W. A. Curtin, Coupled Atomistic and Discrete Dislocation Plasticity, Phys. Rev. Lett. **89**, 025501 (2002).

[88] L. E. Shilkrot, R. E. Miller, and W. A. Curtin, Multiscale plasticity modeling: Coupled atomistics and discrete dislocation mechanics, J. Mech. Phys. Solids **52**, 755 (2004).

[89] X.-S. Kong, X. Wu, Y.-W. You, C. S. Liu, Q. F. Fang, J.-L. Chen, G.-N. Luo, and Z. Wang, First-principles calculations of transition metal-solute interactions with point defects in tungsten, Acta Mater. **66**, 172 (2014).

[90] S. P. Fitzgerald, Crowdion–solute interactions: Analytical modelling and stochastic simulation, Nucl. Instr. Methods Phys. Res. Sec. B **352**, 14 (2015).

[91] M. I. Mendelev and A. H. King, The interactions of self-interstitials with twin boundaries, Philos. Mag. **93**, 1268 (2013).